

Adaptivity for a nonconforming Finite-Element-Method for Maxwell's equations

Diplomarbeit

Humboldt-Universität zu Berlin
Mathematisch-Naturwissenschaftliche Fakultät II
Institut für Mathematik

eingereicht von: Jan Reininghaus
geb.: am 10. Mai 1981
in: Wipperfürth

1. Betreuer: Prof. Dr. Carsten Carstensen
2. Betreuer: Prof. Dr. Susanne C. Brenner

Berlin, den 29. Juni 2007

Contents

0	Introduction	1
1	Mathematical model of electromagnetism	3
1.1	Maxwell's equations	3
1.2	A semi-discretization of Maxwell's equations	4
1.3	The time harmonic form of Maxwell's equations	5
1.4	The boundary value problem	6
2	Existence and uniqueness results for Maxwell's equations	7
2.1	The (reduced) weak form	7
2.2	Existence and uniqueness	8
3	A priori analysis and an error estimator	11
3.1	Motivation for a nonstandard method	11
3.2	A nonconforming Finite-Element-Method	12
3.3	Convergence Analysis	12
3.4	A plausible error estimator	15
4	Numerical implementation and results	17
4.1	Construction of the discrete space	17
4.2	Computation of the global Energy matrix	19
4.3	Numerical results	21
4.3.1	The square domain	21
4.3.2	The L-shape domain	25
4.3.3	The half-L-shape domain	34
5	Theses	43

Chapter 0

Introduction

The numerical solution to Maxwell's equations has an interesting history. Since the original curl-curl formulation of Maxwell's equation is non-elliptic, one first considered the curl-curl minus grad-div ellipticized version. But since it is difficult to construct finite elements that are dense in the space of solutions $X_N := (H_0(\text{curl}; \Omega) \cap H(\text{div}; \Omega))$ of the ellipticized version, the idea to solve Maxwell's equations through it was abandoned (Note that standard P_1 finite elements are not dense in X_N if the domain is not convex and a projection of the solution onto this space does converge to a wrong function). Instead $H(\text{curl}; \Omega)$ conforming elements were developed and the curl-curl problem is solved directly. In recent years however several methods were proposed that employ various ideas to solve the ellipticized version. For example, it was shown that if we augment the standard P_1 finite element space with singular solutions at the corners of the domain, then this space is dense in X_N . One can also regularize the ellipticized version and solve it directly with standard finite elements.

In this Diploma thesis we will present a nonconforming finite element method that was developed recently (see [1] and [2]), the proof that this method produces solutions that converge to the solution of Maxwell's equations, how to efficiently implement this method, some numerical results that corroborate the theoretical predictions, and we propose a plausible error estimator which yields optimal convergence in practice.

For completeness we introduce the reader to the mathematical model of Maxwell's equations that we consider and present an existence and uniqueness proof.

Chapter 1

Mathematical model of electromagnetism

The modern theory of electromagnetism was founded in 1873 by Maxwell with the publication *Treatise on Electricity and Magnetism*. It models the electromagnetic interrelationship between electric fields, magnetic fields, electric charge, and electric current via two pairs of coupled differential equations. The original description by Maxwell does not guarantee uniqueness of the electromagnetic field. To achieve uniqueness one has to include more constitutional equations where there is considerable flexibility. Therefore we carefully state the model we consider. We follow the presentation of the mathematical model presented in [3] and leave out the details that do not apply to our idealized situation.

As the complete Maxwell system is too complex to be rigidly analyzed in this thesis we only consider the time-harmonic form and the time dependent form with an implicit semi discretization in a vacuum with a perfectly conducting boundary in 2D.

1.1 Maxwell's equations

We describe the electromagnetic field by four vector fields depending on position $x \in \mathbb{R}^3$ and time $t \in \mathbb{R}$: the electric field \mathcal{E} , the magnetic field \mathcal{H} , the electric displacement \mathcal{D} and the magnetic induction \mathcal{B} . An electromagnetic field is created by a set of static electric charges and the flow of electric charge called current. We denote the distribution of the charges by a scalar function ρ and the current by a vector field \mathcal{J} .

Maxwell's equations state that the above quantities are related by the following system of partial differential equations:

$$\begin{aligned} \frac{\partial \mathcal{B}}{\partial t} + \nabla \times \mathcal{E} &= 0 && \text{(Faraday's law),} \\ \nabla \cdot \mathcal{D} &= \rho && \text{(Gauss's law),} \\ \frac{\partial \mathcal{D}}{\partial t} - \nabla \times \mathcal{H} &= -\mathcal{J} && \text{(Ampere's law),} \\ \nabla \cdot \mathcal{B} &= 0 && \text{(No magnetic monopoles).} \end{aligned} \tag{1.1}$$

To arrive at a unique description of the electromagnetic field we must relate \mathcal{E} to \mathcal{D} and \mathcal{H} to \mathcal{B} . To do this, we augment the system by two constitutive laws

$$\mathcal{D} = \epsilon \mathcal{E} \text{ and } \mathcal{B} = \mu \mathcal{H}. \quad (1.2)$$

For simplicity we restrict ϵ, μ to be constants, which models vacuum or free space. In this case ϵ is called *electric permittivity* and μ is called *magnetic permeability*. For inhomogeneous, isotropic materials ϵ and μ are scalar functions depending on the space variable x or even matrix valued for anisotropic materials. Note that in a vacuum we have $\sqrt{\mu\epsilon} = c^{-1}$, where c denotes the speed of light in a vacuum.

The last constitutive law that is needed relates \mathcal{J} and \mathcal{E} to the applied current density \mathcal{J}_a . In a conducting material we can assume that Ohms law

$$\mathcal{J} = \sigma \mathcal{E} + \mathcal{J}_a \quad (1.3)$$

holds with σ being the conductivity of the material, provided the field strengths are not large. Note that in a vacuum $\sigma = 0$, and so $\mathcal{J} = \mathcal{J}_a$.

Substituting the above equations into (1.1) yields the system

$$\begin{aligned} \mu \frac{\partial \mathcal{H}}{\partial t} + \nabla \times \mathcal{E} &= 0, \\ \epsilon \nabla \cdot \mathcal{E} &= \rho, \\ \epsilon \frac{\partial \mathcal{E}}{\partial t} - \nabla \times \mathcal{H} &= -\mathcal{J}_a, \\ \mu \nabla \cdot \mathcal{H} &= 0, \end{aligned} \quad (1.4)$$

which describes the electric and magnetic fields for given charge and current densities in a vacuum.

1.2 A semi-discretization of Maxwell's equations

In an implicit semi-discretization of a time dependent problem like (1.4) we approximate the time derivative by an implicit finite difference, i.e.

$$\left(\frac{\partial \mathcal{X}}{\partial t} \right)^{(k)} \approx h^{-1} (\mathcal{X}^{(k)} - \mathcal{X}^{(k-1)}),$$

where $\mathcal{X}^{(k)}$ denotes the value of \mathcal{X} at time step k , and h the granularity of our time discretization.

Replacing the time derivatives in (1.4) by their corresponding approximation we get

$$\begin{aligned} \mu h^{-1} (\mathcal{H}^{(k)} - \mathcal{H}^{(k-1)}) + \nabla \times \mathcal{E}^{(k)} &= 0, \\ \epsilon h^{-1} (\mathcal{E}^{(k)} - \mathcal{E}^{(k-1)}) - \nabla \times \mathcal{H}^{(k)} &= -\mathcal{J}_a. \end{aligned} \quad (1.5)$$

Solving (1.5) for $\mathcal{H}^{(k)}$ and $\mathcal{E}^{(k)}$ yields

$$\begin{aligned}\nabla \times (\nabla \times \mathcal{E}^{(k)}) + \alpha \mathcal{E}^{(k)} &= F, \\ \nabla \times (\nabla \times \mathcal{H}^{(k)}) + \alpha \mathcal{H}^{(k)} &= G,\end{aligned}\tag{1.6}$$

with known data $\alpha = h^{-2}\epsilon\mu$, $F = \alpha\mathcal{E}^{(k-1)} + h^{-1}\mu\nabla \times \mathcal{H}^{(k-1)}$ and $G = \alpha\mathcal{H}^{(k-1)} - h^{-1}\epsilon\nabla \times \mathcal{E}^{(k-1)}$. The type of equation we need to analyze and solve numerically in each time step is therefore

$$\nabla \times (\nabla \times u) + \alpha u = f\tag{1.7}$$

for given data f and $\alpha > 0$.

1.3 The time harmonic form of Maxwell's equations

Using the Fourier transform in time, the time-dependent problem (1.1) can be reduced to the time-harmonic Maxwell system. The electromagnetic field is said to be time-harmonic with temporal frequency $\omega > 0$ provided

$$\mathcal{X}(x, t) = \text{Re}(\exp(-i\omega t)\hat{\mathcal{X}}(x))\tag{1.8}$$

for $\mathcal{X} = \mathcal{E}, \mathcal{H}, \mathcal{D}$ and \mathcal{B} , where $\text{Re}(\cdot)$ denotes the real part of the expression and i denotes the imaginary unit. For consistency reasons we also assume that ρ and \mathcal{J} are of the form (1.8).

Substituting into (1.1) results in the time-harmonic Maxwell equations:

$$\begin{aligned}-i\omega\hat{\mathcal{B}} + \nabla \times \hat{\mathcal{E}} &= 0, \\ \nabla \cdot \hat{\mathcal{D}} &= \hat{\rho}, \\ -i\omega\hat{\mathcal{D}} - \nabla \times \hat{\mathcal{H}} &= -\hat{\mathcal{J}}, \\ \nabla \cdot \hat{\mathcal{B}} &= 0.\end{aligned}\tag{1.9}$$

Note that we can eliminate $\hat{\rho}$ from the system by taking the divergence of (1.9)c.

For convenience we define

$$E = \sqrt{\epsilon}\hat{\mathcal{E}} \quad \text{and} \quad H = \sqrt{\mu}\hat{\mathcal{H}}.\tag{1.10}$$

Incorporating the constitutive relationships (1.2) and (1.3) we arrive at the first order time-harmonic Maxwell system in vacuum:

$$\begin{aligned}-i\kappa H + \nabla \times E &= 0, \\ -i\kappa E - \nabla \times H &= -\frac{1}{i\kappa}F,\end{aligned}\tag{1.11}$$

with $F = i\kappa\sqrt{\mu}\hat{\mathcal{J}}_a$ and the wavenumber $\kappa = \omega\sqrt{\epsilon\mu}$. In this thesis we consider the second order Maxwell system

$$\nabla \times (\nabla \times E) - \kappa^2 E = F,\tag{1.12}$$

which is obtained by solving (1.11)a for H and substituting into (1.11)b. To simplify the situation we assume κ to be real number, so the solution and all involved fields are real. Note that the above equation is similar to (1.7), only now we have $\alpha = -\kappa^2 < 0$.

1.4 The boundary value problem

It remains to discuss the boundary conditions. As we shall see later it is necessary that $\nu \times E$ is well defined along any closed non intersecting curve S with outer normal vector ν and induced partitions $\Omega_1 \cup \Omega_2 = \mathbb{R}^2$, i.e.

$$\nu \times E_1 = \nu \times E_2 \quad \text{on } S, \quad (1.13)$$

where E_1 and E_2 denote the limit of E as it approaches S from Ω_1 respectively Ω_2 . On the other hand, there may be singularities in the charge density ρ , that lead to jumps in the normal component of E across S if ϵ is discontinuous across S . Therefore any numerical scheme that tries to solve (1.12) must ensure that the tangential component is continuous across S , while it must allow jumps of the normal component across S .

In this thesis we will only consider perfectly conducting boundary conditions, the domain Ω on which we want to solve (1.12) consists of a homogeneous material, while its complement $\mathbb{R}^2 \setminus \Omega$ consists of a perfect conductor, i.e. $\sigma \rightarrow \infty$. If the current density \mathcal{J} is to remain bounded, (1.3) implies that the electric field E must vanish outside Ω . With (1.13) we thus arrive at the boundary condition for our model and state the complete boundary value problem that we consider for completeness and future reference:

Given a vectorfield f on a domain Ω , and a constant $\alpha \neq 0$ find the vectorfield u such that

$$\begin{aligned} \nabla \times (\nabla \times u) + \alpha u &= f & \text{in } \Omega, \\ \nu \times u &= 0 & \text{on } \partial\Omega, \end{aligned} \quad (1.14)$$

where ν denotes the outer unit normal of Ω .

Chapter 2

Existence and uniqueness results for Maxwell's equations

In this chapter we present a theory which guarantees existence and uniqueness of a solution to (1.14) under relatively weak assumptions and present the involved function spaces like $H(\text{curl}; \Omega)$ and $H(\text{div}; \Omega)$. In case of $\alpha > 0$ the analysis is a straightforward application of the Riesz representation theorem presented in section 2. In case of $\alpha < 0$ the situation is more difficult. We take an approach based on the Fredholm alternative in section 3 as presented in [3]. For the notation and details of the involved function spaces we refer to [3]. Also we always assume that Ω is a simply connected Lipschitz domain.

2.1 The (reduced) weak form

We derive the weak formulation of (1.14) by multiplying with a test function v that satisfies the boundary condition and integrating over Ω :

$$(\nabla \times (\nabla \times u), v) + \alpha(u, v) = (f, v) \quad (2.1)$$

Here and throughout, (\cdot, \cdot) denotes the $L_2(\Omega)$ scalar product. Partial integration results in the weak form

$$(\nabla \times u, \nabla \times v) + \alpha(u, v) = (f, v) \quad \text{for all } v \in H_0(\text{curl}; \Omega) \quad (2.2)$$

of (1.14), where we use the test space $H_0(\text{curl}; \Omega)$ so that all integrals are well defined when $f \in L_2(\Omega)$ and the boundary condition is fulfilled.

For future reference we state the induced bilinear form $a : H_0(\text{curl}; \Omega) \times H_0(\text{curl}; \Omega) \rightarrow \mathbb{R}$

$$a(u, v) = (\nabla \times u, \nabla \times v) + \alpha(u, v). \quad (2.3)$$

We will now derive the reduced form of (2.2) by splitting the Ansatz and test space into a curl free and a div free part. We need to do this, as the curl of a gradient field is zero, i.e. the involved differential operator has a large null space. To accomplish the splitting we need two

Theorem 2.1 (Helmholtz decompositions) *Let Ω denote a simply connected Lipschitz domain. Then for every $f \in (L_2(\Omega))^2$ there exist $\dot{f} \in H(\text{div}^0; \Omega)$ and $\mu \in H_0(\nabla; \Omega)$ such that*

$$f = \dot{f} + \nabla \mu, \quad (2.4)$$

and for every $u \in H_0(\text{curl}; \Omega)$ there exist unique $\dot{u} \in (H_0(\text{curl}; \Omega) \cap H(\text{div}^0; \Omega))$ and $\phi \in H_0(\nabla; \Omega)$ such that

$$u = \dot{u} + \nabla \phi. \quad (2.5)$$

Inserting (2.5) into (2.2) results in

$$(\nabla \times (\dot{u} + \nabla \phi), \nabla \times v) + \alpha((\dot{u} + \nabla \phi), v) = (f, v) \quad \text{for all } v \in H_0(\text{curl}; \Omega). \quad (2.6)$$

As $\nabla H_0(\nabla; \Omega) \subset H_0(\text{curl}; \Omega)$ we can choose $v = \nabla \psi$:

$$\begin{aligned} (\nabla \times (\dot{u} + \nabla \phi), \nabla \times \nabla \psi) + \alpha((\dot{u} + \nabla \phi), \nabla \psi) &= (f, \nabla \psi) \\ \iff \alpha(\nabla \phi, \nabla \psi) &= (f, \nabla \psi), \end{aligned} \quad (2.7)$$

i.e. ϕ is the solution of a Laplace equation whose uniqueness, existence and computation are well understood. If we insert the Helmholtz decompositions $u = \dot{u} + \nabla \phi$, $v = \dot{v} + \nabla \psi$ and $f = \dot{f} + \nabla \mu$ into (2.3) we get:

$$\begin{aligned} (\nabla \times (\dot{u} + \nabla \phi), \nabla \times (\dot{v} + \nabla \psi)) + \alpha(\dot{u} + \nabla \phi, \dot{v} + \nabla \psi) &= (\dot{f} + \nabla \mu, \dot{v} + \nabla \psi) \\ \iff (\nabla \times \dot{u}, \nabla \times \dot{v}) + \alpha(\dot{u}, \dot{v}) + \alpha(\nabla \phi, \nabla \psi) &= (f, \nabla \psi) + (\dot{f} + \nabla \mu, \dot{v}) \\ \iff (\nabla \times \dot{u}, \nabla \times \dot{v}) + \alpha(\dot{u}, \dot{v}) &= (\dot{f}, \dot{v}). \end{aligned} \quad (2.8)$$

Note that the above weak form is of the same form as (1.14), only the right hand side and the test space changed. From here on the basis for our analysis and the numerical scheme will therefore be the

Definition 2.2 (Reduced weak form of Maxwell's equations) *Given a vectorfield $f \in H(\text{div}^0; \Omega)$ on a simply connected Lipschitz domain Ω , and a constant $\alpha \neq 0$ find the vectorfield $u \in V := (H_0(\text{curl}; \Omega) \cap H(\text{div}^0; \Omega))$ such that*

$$(\nabla \times u, \nabla \times v) + \alpha(u, v) = (f, v) \quad \text{for all } v \in V. \quad (2.9)$$

2.2 Existence and uniqueness

Let us first consider the case of $\alpha > 0$. We show that the left hand side of (2.9) defines a scalar product on V to apply the

Theorem 2.3 (Riesz representation theorem) *Let V be a Hilbert space with scalar product $a : V \times V \rightarrow \mathbb{R}$ and let $F \in V^*$. Then there exists a unique $v \in V$ such that*

$$a(u, v) = F(v) \quad \text{for all } v \in V.$$

Symmetry and linearity follow directly from the definition. Positive definiteness is also clear as $\alpha > 0$:

$$a(u, u) = (\nabla \times u, \nabla \times u) + \alpha(u, u) \geq \alpha(u, u) = 0 \quad \text{if and only if } u = 0.$$

But note that with this approach the ellipticity constant is α , which may lead to problems in the numerical algorithm for certain applications. This is where the decomposition of $H_0(\text{curl}; \Omega)$ proves useful as we have a

Theorem 2.4 (Friedrichs inequality) *Let u be a function in $H_0(\text{curl}; \Omega) \cap H(\text{div}; \Omega)$. Then the inequality*

$$(u, u) \leq C \left((\nabla \times u, \nabla \times u) + (\nabla \cdot u, \nabla \cdot u) \right) \quad (2.10)$$

holds, where $C > 0$ is a constant depending only on Ω .

As u belongs to $H_0(\text{curl}; \Omega) \cap H(\text{div}; \Omega)$ we see that the bilinear form $a(\cdot, \cdot)$ has an ellipticity constant of $\alpha + \frac{1}{C} > 0$, i.e. it is bounded away from 0 as $\alpha \searrow 0$.

When α is negative the situation is a lot more complex. If $\alpha + \frac{1}{C} > 0$, where C is the constant from (2.10), then the bilinear form $a(\cdot, \cdot)$ defines a scalar product and we can apply theorem 2.3, but in general this is not the case. To show existence and uniqueness we first define the corresponding operator equation, show that it is of Fredholm type, i.e. uniqueness implies existence, and can therefore finish by showing uniqueness of the solution.

We start by defining the bilinear form

$$a_+(u, v) = (\nabla \times u, \nabla \times v) - \alpha(u, v).$$

Since for $\alpha < 0$ the above bilinear form defines a scalar product, we can define the operator $K : (L_2(\Omega))^2 \rightarrow (L_2(\Omega))^2$ implicitly by requiring that

$$a_+(K(f), v) = 2\alpha(f, v) \quad \text{for all } v \in V,$$

as the Riesz representation theorem applies. K can be thought of as the solution operator for the coercive version of (2.9) with a modified right hand side. One can now show that K is a bounded and compact operator from $(L_2(\Omega))^2$ to $(L_2(\Omega))^2$. We proceed by defining the right hand side F of our operator equation implicitly by

$$a_+(F, v) = (f, v) \quad \text{for all } v \in V,$$

i.e. F is the solution of the coercive version of (2.9).

We can now state (2.9) equivalently as an operator equation: Find $u \in (L_2(\Omega))^2$ such that

$$(I + K)u = F.$$

Since K is compact we can apply the

Theorem 2.5 (Fredholm Alternative) *Let K be a linear, bounded and compact operator on a Hilbert space H and let I denote the identity operator. Then the homogeneous equation $(I + K)u = 0$ has either $p > 0$ linear independent solutions or the inhomogeneous equation $(I + K)u = F$ has a unique solution which depends continuously on the right hand side F for every $F \in H$.*

We now need to show that (2.9) has at most one solution to guarantee existence. This is only the case, when α is not an eigenvalue of the problem

$$(\nabla \times u, \nabla \times v) = -\alpha(u, v). \quad (2.11)$$

We define the operator $L : (L_2(\Omega))^2 \rightarrow (L_2(\Omega))^2$ implicitly by requiring that

$$a(Lf, v) = (f, v) \quad \text{for all } v \in V.$$

Since this operator is compact and self-adjoint on $L_2(\Omega)$ we can apply the Hilbert-Schmidt Eigenvalue theory, i.e. we can show that the equation (2.11) can have a discrete set of eigenvalues with corresponding non trivial eigenfunctions. If α is such an eigenvalue we can neither expect uniqueness or even existence of a solution for the problem (2.9), but as the set of eigenvalues is discrete this is almost never the case and we thus arrive at the concluding theorem that shows

Theorem 2.6 (Existence and uniqueness for Maxwell's equations) *Let f be a function in $(L_2(\Omega))^2$ and let $\alpha \neq 0$ be a real number that is not a Maxwell eigenvalue. Then there exists a unique $u \in H_0(\text{curl}; \Omega)$ such that*

$$(\nabla \times u, \nabla \times v) + \alpha(u, v) = (f, v) \quad \text{for all } v \in H_0(\text{curl}; \Omega) \quad (2.12)$$

In the remaining chapters we will consider an ellipticized version of the reduced form of Maxwell's equations. As in the reduced form the solution u is in $H(\text{div}^0; \Omega)$ we can add $(\nabla \cdot u, \nabla \cdot v)$ to the bilinear form without changing the exact solution. This leads to

Theorem 2.7 (Existence and uniqueness for the reduced ellipticized form) *Let f be a function in $H(\text{div}^0; \Omega)$ and let $\alpha \neq 0$ be a real number that is not an eigenvalue of (2.13). Then there exists a unique $u \in V := (H_0(\text{curl}; \Omega) \cap H(\text{div}; \Omega))$ such that*

$$(\nabla \times u, \nabla \times v) + (\nabla \cdot u, \nabla \cdot v) + \alpha(u, v) = (f, v) \quad \text{for all } v \in V \quad (2.13)$$

Chapter 3

A priori analysis and an error estimator

We will present a converging scheme for an ellipticized version of (2.9) that is proposed in [2]. First we present a motivation as to why nonstandard finite elements have to be employed if Ω is not convex. Then we introduce a nonconforming method which will be analysed in detail followed by a convergence proof. We finish the chapter by proposing a plausible error estimator which numerically seems to be reliable and locally efficient as shown in chapter 4.

3.1 Motivation for a nonstandard method

To understand why a P_1 conforming FEM does not work in this setting we present the following description of the space in which the solution exists:

$$V := (H_0(\text{curl}; \Omega) \cap H(\text{div}^0; \Omega)) = H(\nabla; \Omega) + \nabla(\Delta^{-1}(L_2(\Omega))), \quad (3.1)$$

where $\nabla(\Delta^{-1}(L_2(\Omega)))$ denotes the gradient of a solution of a Laplace problem with homogeneous boundary conditions on Ω . From the regularity theory of the Laplace problem we know that if Ω is convex, then the gradient of a solution v is in $H(\nabla; \Omega)$. This shows, that the solution space is the same as $H(\nabla; \Omega)$ if Ω is convex, and standard conforming methods like P_1 can be employed. If however, Ω is not convex, then the gradient of a solution of the Laplace problem is not in $H(\nabla; \Omega)$ (see figure 4.6, for an example). One can show that $H(\nabla; \Omega)$ is a closed subspace of V with infinite codimension if Ω is not convex. This explains why standard methods converge to a function that has a positive distance from the real solution as one really approximates the $H(\nabla; \Omega)$ projection of a function that is not in $H(\nabla; \Omega)$.

Here, we propose a nonconforming method to be able to compute reliably solutions for Maxwell's equations on general (non convex) domains. The discrete space we use consists of piecewise affine vector fields, where continuity is only enforced at the midpoints of the edges of the mesh. Note that in the scalar case the gradient operator takes care of the consistency error, i.e. it is not necessary to take care of the jumps in the bilinear form. For Maxwell's equations however, the differential operator is not strong enough to reduce the inconsistency error and we have to

include the error in our bilinear form to reduce it as the mesh gets finer. As the solution may contain singular parts at the corners of the domain, we need to apply an appropriate weight to the consistency error in the bilinear form.

3.2 A nonconforming Finite-Element-Method

The numerical method we consider is to find $u_h \in V_h$ such that

$$a_h(u_h, v) = (f, v) \quad \forall v \in V_h \quad (3.2)$$

where

$$\begin{aligned} a_h(w, v) = & (\nabla_h \times w, \nabla_h \times v) + (\nabla_h \cdot w, \nabla_h \cdot v) + \alpha(w, v) \\ & + \sum_{e \in \mathcal{E}_h} \frac{\Phi_\mu(e)^2}{h_e} (J(n_e \times w), J(n_e \times v))_e + \sum_{e \in \mathcal{E}_h^i} \frac{\Phi_\mu(e)^2}{h_e} (J(n_e \cdot w), J(n_e \cdot v))_e \end{aligned} \quad (3.3)$$

where $\Phi_\mu(e) = \prod_{\ell=1}^L |c_\ell - m_\ell|^{1-\mu_\ell}$ is a weight function depending on grading parameters μ for the corners c_ℓ of Ω . The choice of μ_ℓ is determined by the internal angle ω_ℓ of Ω at c_ℓ . We set $\mu_\ell = 1$ if $\omega_\ell \leq \frac{\pi}{2}$ and $\mu_\ell = \frac{\pi}{2\omega_\ell}$ otherwise. Here V_h consists of piecewise affine functions that are continuous at the midpoints of the edges of \mathcal{T} and whose tangential component vanishes at the midpoints along $\partial\Omega$ and $J(\cdot)$ denotes the jump operator.

We will measure the error of the approximate solution by the norm

$$\begin{aligned} \|v\|_h^2 = & \|\nabla_h \times v\|^2 + \|\nabla_h \cdot v\|^2 + \|v\|^2 \\ & + \sum_{e \in \mathcal{E}_h} \frac{\Phi_\mu(e)^2}{h_e} \|[n_e \times v]\|_e^2 + \sum_{e \in \mathcal{E}_h^i} \frac{\Phi_\mu(e)^2}{h_e} \|[n_e \cdot v]\|_e^2. \end{aligned} \quad (3.4)$$

3.3 Convergence Analysis

The goal of this section is to derive optimal convergence of the method on graded meshes. The method we consider here is the one presented in [2], although we only consider $f \in H(\text{div}^0; \Omega)$. In [2] it is only assumed that $f \in L_2(\Omega)$, so all theorems and lemmatas that are proven in [2] apply to our case. We therefore limit the detail of the theorems and proofs and only present the core elements of the convergence proof.

Note that

$$\|v\|_{L_2(\Omega)} \leq \|v\|_h \quad \forall v \in V + V_h \quad (3.5)$$

and

$$|a_h(w, v)| \leq (|\alpha| + 1) \|w_h\| \|v\|_h \quad \forall v \in V + V_h. \quad (3.6)$$

We start by presenting two abstract error estimates:

Lemma 3.1 (Abstract error estimate for $\alpha > 0$) *Let $\alpha > 0$, $\beta = \min(1, \alpha)$, u a solution to (2.13), and let u_h satisfy (3.2). Then we have*

$$\|u - u_h\|_h \leq \frac{1 + \alpha + \beta}{\beta} \inf_{v \in V_h} \|u - v\|_h + \frac{1}{\beta} \max_{w \in V_h \setminus 0} \frac{a_h(u - u_h, w)}{\|w\|_h} \quad (3.7)$$

The proof of this lemma makes use of (3.6), a triangle inequality, and of the coercivity of the bilinear form when $\alpha > 0$, i.e.

$$a_h(v, v) \geq \min(1, \alpha) \|v_h\|^2 \quad (3.8)$$

Lemma 3.2 (Abstract error estimate for $\alpha < 0$) *Let $\alpha < 0$, u a solution of (2.13), and let u_h satisfy (3.2). Then we have*

$$\|u - u_h\|_h \leq (2|\alpha| + 3) \inf_{v \in V_h} \|u - v\|_h + \max_{w \in V_h \setminus 0} \frac{a_h(u - u_h, w)}{\|w\|_h} + (|\alpha| + 1) \|u - u_h\|_{L_2(\Omega)} \quad (3.9)$$

To proof this lemma, one can use (3.5), (3.6), a triangle inequality, and the equality

$$a_h(v, v) + (|\alpha| + 1)(v, v) = \|v\|_h^2, \quad (3.10)$$

which holds for $\alpha \leq 0$.

The first term of the right hand sides of (3.2) and (3.1) measures the approximation property of the discrete space V_h , the second term measures the consistency error due to the non conformity of V_h , and the third term of (3.2) is due to the indefiniteness of the discrete problem when $\alpha \leq 0$. We continue by defining the natural weak interpolation operator $\Pi_T : (H^s(T)) \rightarrow (P_1(T))^2$ for $s > \frac{1}{2}$ by

$$(\Pi_T)\xi(m_{e_i}) = \frac{1}{|e_i|} \int_{e_i} \xi$$

The global interpolation operator $\Pi_T : (H^s(T)) \rightarrow V_h$ is then defined by

$$(\Pi_h u)_T = \Pi_T u_T \quad \forall T \in \mathcal{T}$$

On properly graded meshes (see [1]) one can then show the following

Lemma 3.3 (Interpolation error estimates) *Let u be the solution of (2.13). Then we have*

$$\|u - \Pi_h u\|_{L_2(\Omega)} \leq C_\epsilon h^{2-\epsilon} \|f\|_{L_2(\Omega)}, \quad (3.11)$$

$$\sum_{e \in \mathcal{E}_h} \|J(u - \Pi_h u)\|_{L_2(e)}^2 \leq C_\epsilon h^{2-\epsilon} \|f\|_{L_2(\Omega)}, \quad (3.12)$$

for any $\epsilon > 0$.

We can now estimate the terms that appear in the abstract error estimates (3.1) and (3.2).

Lemma 3.4 (Approximation error) *Let u denote the solution of (2.13). It holds that*

$$\inf_{v \in V_h} \|u - v\|_h \leq \|u - \Pi_h u\|_h \leq C_\epsilon h^{1-\epsilon} \|f\|_{L_2(\Omega)}, \quad (3.13)$$

for any $\epsilon > 0$.

Lemma 3.5 (Consistency error) *Let u denote the solution of (2.13) and let $u_h \in V_h$ satisfy (3.2). We then have*

$$\max_{w \in V_h \setminus 0} \frac{a_h(u - u_h, w)}{\|w\|_h} \leq Ch \|f\|_{L_2(\Omega)}. \quad (3.14)$$

Lemma 3.6 (Indefiniteness error) *Let u denote the solution of (2.13) and let $u_h \in V_h$ satisfy (3.2). It holds that*

$$\|u - u_h\|_{L_2(\Omega)} \leq C_\epsilon (h^{2-\epsilon} \|f\|_{L_2(\Omega)} + h^{1-\epsilon} \|u - u_h\|_h). \quad (3.15)$$

We can now prove convergence of the scheme. In the case of $\alpha > 0$ this follows immediately from the lemmata 3.1, 3.4, and 3.5.

Theorem 3.7 (Convergence result for $\alpha > 0$) *Let u denote the solution of (2.13), $u_h \in V_h$ satisfy (3.2) and $\alpha > 0$. Then the following estimates hold for any ϵ :*

$$\|u - u_h\|_h \leq C_\epsilon h^{1-\epsilon} \|f\|_{L_2(\Omega)}, \quad (3.16)$$

$$\|u - u_h\|_{L_2(\Omega)} \leq C_\epsilon h^{2-\epsilon} \|f\|_{L_2(\Omega)}. \quad (3.17)$$

If α is not positive, then we can only show that the discrete problem is uniquely solvable for all meshes with $h < h^*$ (see figures 4.15 and 4.16) as is stated in the following

Theorem 3.8 (Convergence result for $\alpha \leq 0$) *Let u denote the solution of (2.13) and let ϵ denote an arbitrary positive real number. Assuming that $-\alpha$ is not an eigenvalue of the homogeneous version of (2.13) there exists a mesh granularity h^* (depending on ϵ) such that the discrete problem (3.2) has a unique solution for all $h < h^*$ and we have:*

$$\|u - u_h\|_h \leq C_\epsilon h^{1-\epsilon} \|f\|_{L_2(\Omega)}, \quad (3.18)$$

$$\|u - u_h\|_{L_2(\Omega)} \leq C_\epsilon h^{2-\epsilon} \|f\|_{L_2(\Omega)}. \quad (3.19)$$

To prove this main result we employ the abstract error estimate 3.2 and the estimates 3.1, 3.4, and 3.5. Assuming u_h satisfies (2.13) this leads to

$$\|u - u_h\|_h \leq C_\epsilon h^{1-\epsilon} (\|f\|_{L_2(\Omega)} + \|u - u_h\|_h). \quad (3.20)$$

For a fixed ϵ we can now set $h^* := \frac{1}{(2C_\epsilon)^{1/(1-\epsilon)}}$. Then we have for all $h < h^*$

$$\|u - u_h\|_h \leq C_\epsilon h^{1-\epsilon} \|f\|_{L_2(\Omega)} + \frac{1}{2} \|u - u_h\|_h. \quad (3.21)$$

If $z \in V_h$ is a solution of the homogeneous version of (2.13) we can therefore deduce $\|z\|_h \leq 0$, i.e. $z = 0$. This means that the discrete problem is uniquely solvable for $h \leq h^*$. The given estimates then follow from (3.21) and 3.5

3.4 A plausible error estimator

As the solution to Maxwell's equations can have singularities (even on convex domains) the underlying mesh of the discrete space needs to be properly managed. One can use graded meshes to achieve optimal convergence rates. However, there are some disadvantages to this approach. Firstly, it is apriori not clear whether there exists a singularity at a certain corner of the domain, and a graded mesh may produce worse solutions than uniform refinement if there is no singularity. Secondly, the singular part of the solution may be very small, and refinement in the interior of the domain may yield better discrete solutions. Asymptotically however, a graded mesh will eventually outperform uniform refinement in such a case.

To overcome these drawbacks one can use an error estimator that indicates where the mesh should be refined. If the error estimator is locally efficient, such a refinement does produce the best results in almost all cases.

We therefore propose the following error estimator $E : V_h \rightarrow \mathbb{R}$ which yields optimal results in practice:

$$\begin{aligned} E(u_h)^2 = & \sum_{T \in \mathcal{T}_h} h_T^2 \|f - \alpha u_h\|_T^2 + \sum_{e \in \mathcal{E}_h} h_e \|J(\nabla \cdot u_h)\|_e^2 + \sum_{e \in \mathcal{E}_h} h_e \|J(\nabla \times u_h)\|_e^2 \\ & + \sum_{e \in \mathcal{E}_h} \frac{\Phi_\mu(e)^2}{h_e} \|J(n_e \times u_h)\|_e^2 + \sum_{e \in \mathcal{E}_h^i} \frac{\Phi_\mu(e)^2}{h_e} \|J(n_e \cdot u_h)\|_e^2, \end{aligned} \quad (3.22)$$

where $J(\cdot)$ denotes the jump operator and n_e the outer unit normal of edge e .

Chapter 4

Numerical implementation and results

In this chapter we present a numerical implementation and results of the method presented in chapter 3. The first section shows how one can efficiently construct the involved discrete space. In section 2, we compute the discrete version of the bilinear form where the emphasis lies on the computation of the jump terms. The last section presents some numerical results that corroborate the theoretical predictions of chapter 3.

4.1 Construction of the discrete space

We want to discretize the space of piecewise linear vector fields, that are continuous at the midpoints of the edges of the mesh, and whose tangential component is zero at the midpoints of all edges of the boundary of the domain Ω . We call this space V_h .

The continuity requirement in the interior of the domain is the same as the in Crouzeix-Raviart nonconforming finite element, which one may already have encountered. In the Crouzeix-Raviart element, the degrees of freedom consist of point evaluations at the midpoints of the edges of the mesh. There are two disadvantages using this standard approach. First, the differential operator cannot be naturally represented using these degrees of freedom. The approach we present below has a natural curl and div representation which will become clear when we compute the global energy matrix in section 2. The simple representation results in a simpler structure of the linear systems of equations that we have to solve. Secondly the boundary conditions cannot be easily implemented with these degrees of freedom, as the tangential component at the midpoint of an edge is determined by two degrees of freedom.

Both of these disadvantages can be resolved, but instead we will now present an alternative approach where the degrees of freedom are the tangential and the normal component at the midpoints of the edges of the mesh. Formally the local degrees of freedom $\xi_1, \dots, \xi_6 \in V_h^*$ for a triangle $T \in \mathcal{T}$ with edges E_i and corresponding globally chosen (i.e. each edge is assigned a unique normal where boundary edges are assigned the normal that points outwards) unit

normals ν_i are given by

$$\begin{aligned}\xi_1(\Phi) &= \nu_1 \times \Phi(M_1), & \xi_2(\Phi) &= \nu_2 \times \Phi(M_2), & \xi_3(\Phi) &= \nu_3 \times \Phi(M_3), \\ \xi_4(\Phi) &= \nu_1 \cdot \Phi(M_1), & \xi_5(\Phi) &= \nu_2 \cdot \Phi(M_2), & \xi_6(\Phi) &= \nu_3 \cdot \Phi(M_3),\end{aligned}\tag{4.1}$$

where

$$\Phi = \sum_{k=1}^6 a_k \phi_k \tag{4.2}$$

is an arbitrary function in $(P_1(T))^2$ and M_i denotes the midpoint of edge i .

Note that although the basis functions ϕ_i can be chosen arbitrarily as long as they form a basis for $(P_1(T))^2$ it is computationally better to choose

$$\begin{aligned}\phi_1 &= (\lambda_1, 0), & \phi_4 &= (0, \lambda_1), \\ \phi_2 &= (\lambda_2, 0), & \phi_5 &= (0, \lambda_2), \\ \phi_3 &= (\lambda_3, 0), & \phi_6 &= (0, \lambda_3),\end{aligned}\tag{4.3}$$

where the λ_i denote the standard basis functions for $P_1(T)$, i.e. when N_i denotes the i th vertex of T we have $\lambda_i(P_j) = \delta_{ij}$.

If we take the degrees of freedom (4.1) as the basis for the space V_h^* both of the aforementioned problems are dealt with: the boundary conditions are represented by a single degree of freedom for each edge and the differential operator has a natural representation as can be seen in section 2 of this chapter.

To finish the construction of the discrete space, we need to compute a basis of V_h that represents the set of degrees of freedom. To do this we compute a basis B of V_h such that the set of degrees of freedom (4.1) is the dual basis of B , i.e. we need to find functions $v_i \in V_h$ with the property $\xi_j(v_i) = \delta_{ij}$. To do this we substitute (4.2) into (4.1) and evaluate the resulting equations using (4.3). When one enumerates the edges of T counterclockwise beginning with the edge that starts in N_1 one gets the system of equations

$$C(T) a = \frac{1}{2} \begin{pmatrix} -\nu_2 & -\nu_2 & 0 & \nu_1 & \nu_1 & 0 \\ 0 & -\nu_2 & -\nu_2 & 0 & \nu_1 & \nu_1 \\ -\nu_2 & 0 & -\nu_2 & \nu_1 & 0 & \nu_1 \\ \nu_1 & \nu_1 & 0 & \nu_2 & \nu_2 & 0 \\ 0 & \nu_1 & \nu_1 & 0 & \nu_2 & \nu_2 \\ \nu_1 & 0 & \nu_1 & \nu_2 & 0 & \nu_2 \end{pmatrix} \begin{pmatrix} a_1 \\ a_2 \\ a_3 \\ a_4 \\ a_5 \\ a_6 \end{pmatrix} = \begin{pmatrix} \xi_1 \\ \xi_2 \\ \xi_3 \\ \xi_4 \\ \xi_5 \\ \xi_6 \end{pmatrix}. \tag{4.4}$$

If one solves this system with $\xi_i = \delta_{ij}$ one gets the coefficients a_i for the basis function that represents ξ_j . To get the dual basis of (4.1) one therefore has to invert the matrix C_T defined in (4.4). The i th column of that inverse denoted by $C_i^{-1}(T)$ then gives the coefficients of the elements ψ_i of the basis B . The union of those functions for all triangles therefore spans the space V_h in a way that is orthonormal with respect to the set of degrees of freedom (4.1).

4.2 Computation of the global Energy matrix

We need to evaluate the bilinear form

$$\begin{aligned} a_h(w, v) = & (\nabla_h \times w, \nabla_h \times v) + (\nabla_h \cdot w, \nabla_h \cdot v) + \alpha(w, v) \\ & + \sum_{E \in \mathcal{E}_h} \frac{1}{|E|} (J(\nu_E \times w), J(\nu_E \times v))_E + \sum_{E \in \mathcal{E}_h^i} \frac{\Phi_\mu(E)^2}{|E|} (J(\nu_E \cdot w), J(\nu_E \cdot v))_E \end{aligned} \quad (4.5)$$

for all functions w, v of the basis B of V_h . As usual, it suffices to compute the bilinear form locally, that is, we compute $(\cdot, \cdot)_T$ for all triangles $T \in \mathcal{T}$ and $(\cdot, \cdot)_E$ for all edges $E \in \mathcal{E}$ and then assemble the global energy matrix. We begin by computing the local energy matrices for the triangles. Note that because of the choice of the basis of V_h the dimension of these matrices is 6×6 .

As the divergence of a linear vector field is a constant we have

$$(\nabla \cdot v, \nabla \cdot w) = |T| \nabla \cdot v \nabla \cdot w$$

To compute $\nabla \cdot v$ and $\nabla \cdot w$ we make use of a simple form of

Theorem 4.1 (Gauss's divergence theorem) *Let $v \in H(\text{div}; \Omega)$ and let ν denote the outer unit normal of Ω . Then*

$$(\nabla \cdot v, 1)_\Omega = (\nu \cdot v, 1)_{\partial\Omega}.$$

If for example v denotes the function that represents ξ_5 we have

$$\nabla \cdot v = |T|^{-1} (\nabla \cdot v, 1)_T = |T|^{-1} (\nu \cdot v, 1)_{\partial T} = |T|^{-1} \sum_{k=1}^3 (\nu \cdot v, 1)_{E_k} = |T|^{-1} |E_2|, \quad (4.6)$$

because the integrals over the edges can be calculated exactly by evaluating the function at the midpoints of the edges.

The local (div, div) matrix reads therefore:

$$(\nabla \cdot \psi_i, \nabla \cdot \psi_j) = \begin{cases} 0 & \text{if } i \leq 3 \text{ or } j \leq 3 \\ |T|^{-1} |E_{i-3}| |E_{j-3}| & \text{otherwise} \end{cases}$$

To compute the local (curl, curl) matrix we follow the same approach, only now we need

Theorem 4.2 (Stokes' theorem) *Let $v \in H(\text{curl}; \Omega)$ and let ν denote the outer unit normal of Ω . Then*

$$(\nabla \times v, 1)_\Omega = (\nu \times v, 1)_{\partial\Omega}.$$

Similarly to the way we used theorem 4.1 in (4.6) we employ the above theorem to get

$$(\nabla \times \psi_i, \nabla \times \psi_j) = \begin{cases} 0 & \text{if } i \geq 4 \text{ or } j \geq 4 \\ |T|^{-1} |E_i| |E_j| & \text{otherwise} \end{cases}$$

To compute the local mass matrix (v, w) we note that

$$\psi_i = C_i^{-1}(T) \cdot (\phi_1, \dots, \phi_6)^T,$$

where $C_i^{-1}(T)$ is defined by (4.4) and ϕ_j by (4.3). The mass term is then given by

$$(\psi_i, \psi_j) = (C_i^{-1}(T) (\phi_1, \dots, \phi_6), C_j^{-1}(T) \cdot (\phi_1, \dots, \phi_6)). \quad (4.7)$$

A simple reordering of the terms involved leads to the following representation of the local mass matrix:

$$(\psi_i, \psi_j) = C_i^{-1}(T)^T \{(\phi_\ell, \phi_k)\}_{\ell,k} C_j^{-1}(T) \quad (4.8)$$

Note that the 6×6 matrix $\{(\phi_\ell, \phi_k)\}_{\ell,k}$ can be easily evaluated exactly because of the choice we made in (4.3):

$$\{(\phi_\ell, \phi_k)\}_{\ell,k} = \frac{|T|}{12} \begin{pmatrix} 2 & 1 & 1 & 0 & 0 & 0 \\ 1 & 2 & 1 & 0 & 0 & 0 \\ 1 & 1 & 2 & 0 & 0 & 0 \\ 0 & 0 & 0 & 2 & 1 & 1 \\ 0 & 0 & 0 & 1 & 2 & 1 \\ 0 & 0 & 0 & 1 & 1 & 2 \end{pmatrix} = M_{P_1^2}$$

The complete local mass matrix is thus given by

$$(\psi_i, \psi_j) = C(T)^T M_{P_1^2} C(T).$$

It remains to discuss the jump terms of the bilinear form. Here, we follow the same approach as with the standard element-wise terms, only now we loop over the edges of the mesh. Note that the dimension of these local edge matrices is 10×10 , as we need to consider all degrees of freedom that are nonzero on the edge, i.e. we need to consider the edge patch $T_1 \cap T_2 = E$. We enumerate the degrees of freedom locally in the following way: $\xi_{1,\dots,4}$ represent the degrees of freedom whose support is in T_1 , $\xi_{5,\dots,8}$ represent the degrees of freedom whose support is in T_2 and ξ_9, ξ_{10} represent the degrees of freedom whose support is equal to $T_1 \cup T_2$. Note that ξ_9 and ξ_{10} do not jump over the edge, and we can reduce the dimension of the local edge matrix to 8×8 .

We now show how the normal jump can be computed in the interior. The other jump terms can be computed analogously. For $i \leq 4$ and $j \leq 4$ we have

$$\begin{aligned} (J(\nu_E \cdot \psi_i), J(\nu_E \cdot \psi_j))_E &= (\nu_E \cdot \psi_i, \nu_E \cdot \psi_j)_E \\ &= (\nu_E \cdot \sum_{k=1}^6 C_{k,i}^{-1}(T_1) \phi_k, \nu_E \cdot \sum_{\ell=1}^6 C_{\ell,j}^{-1}(T_1) \phi_\ell)_E \\ &= \sum_{k=1}^6 \sum_{\ell=1}^6 C_{k,i}^{-1}(T_1) (\nu_E \cdot \phi_k, \nu_E \cdot \phi_\ell)_E C_{\ell,j}^{-1}(T_1) \end{aligned} \quad (4.9)$$

As $\phi_k^T \phi_\ell \in \mathbb{R}^{2 \times 2}$ has only one nonzero entry, a direct calculation leads to the expression

$$(J(\nu \cdot \psi_i), J(\nu \cdot \psi_j))_E = \begin{cases} (C^{-1}(T_1))^T N M_{T_1, T_1} N C^{-1}(T_1) & \text{if } i \leq 4 \text{ and } j \leq 4 \\ (C^{-1}(T_1))^T (-N) M_{T_1, T_2} N C^{-1}(T_2) & \text{if } i \leq 4 \text{ and } j \geq 5 \\ (C^{-1}(T_2))^T N M_{T_2, T_1} (-N) C^{-1}(T_1) & \text{if } i \geq 5 \text{ and } j \leq 4 \\ (C^{-1}(T_2))^T (-N) M_{T_2, T_2} (-N) C^{-1}(T_2) & \text{if } i \geq 5 \text{ and } j \geq 5 \end{cases},$$

where

$$N = \begin{pmatrix} \nu_1 & 0 & 0 & 0 & 0 & 0 \\ 0 & \nu_1 & 0 & 0 & 0 & 0 \\ 0 & 0 & \nu_1 & 0 & 0 & 0 \\ 0 & 0 & 0 & \nu_2 & 0 & 0 \\ 0 & 0 & 0 & 0 & \nu_2 & 0 \\ 0 & 0 & 0 & 0 & 0 & \nu_2 \end{pmatrix},$$

and M_{T_k, T_ℓ} represents the local edge mass matrix $(\phi_i, \phi_j)_E$ where $\phi_i = 0$ on T_ℓ and $\phi_j = 0$ on T_k . For example, let the edge E be the first edge locally in both triangles, then

$$M_{T_1, T_1} = \frac{|E|}{6} \begin{pmatrix} 2 & 1 & 0 & 0 & 0 & 0 \\ 1 & 2 & 0 & 0 & 0 & 0 \\ 0 & 0 & 0 & 0 & 0 & 0 \\ 0 & 0 & 0 & 2 & 1 & 0 \\ 0 & 0 & 0 & 1 & 2 & 0 \\ 0 & 0 & 0 & 0 & 0 & 0 \end{pmatrix}.$$

The other cases then result by a permutation of the columns and rows of the above matrix depending on the local edge numbers of both triangles.

4.3 Numerical results

In this section we will present some numerical results that corroborate the theoretical predictions from chapter 3. We discuss three different domains that model the different regularity presented in [1]: a square for regular solutions, an L-shape domain, as an example of a domain with an interior angle $\omega \geq \frac{3\pi}{2}$, and finally a convex domain exhibiting an angle $\frac{\pi}{2} < \omega < \pi$ called half-L-shape.

For all domains, we specify a representative exact solution and compute the corresponding right hand side symbolically to be able to compute the exact error. On the L-shape and half-L-shape domains we also compute discrete solutions for a right hand side $f \equiv 1$. To illustrate the suboptimal convergence order of uniform refinement on the half-L-shape, we also include an example with non-homogeneous boundary.

All involved integrals that cannot be computed exactly are evaluated with Gauss quadrature of order 19 on each triangle. The error graphs are plotted in a log-log scale to illustrate the convergence rate, where the x-axis represents the number of degrees of freedom and the y-axis the error.

4.3.1 The square domain

We consider the function

$$u = \begin{pmatrix} y(y-1) \sin(\pi y) \\ x(x-1) \sin(\pi x) \end{pmatrix} \quad (4.10)$$

on $\Omega = [0, 1]^2$ and compute u_h for several values of the parameter α . As the function is very regular, we only compute the solution on uniform meshes. All error graphs exhibit an optimal

convergence behavior of h^2 , respectively h , and the asymptotic error seems to be independent of α .

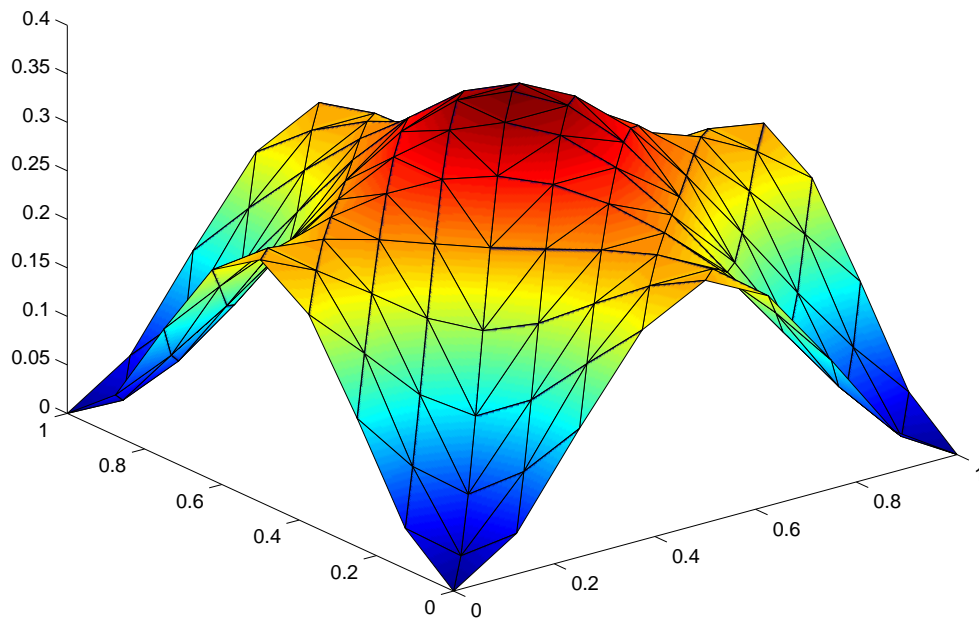


Figure 4.1: Norm of the exact solution of example (4.10)

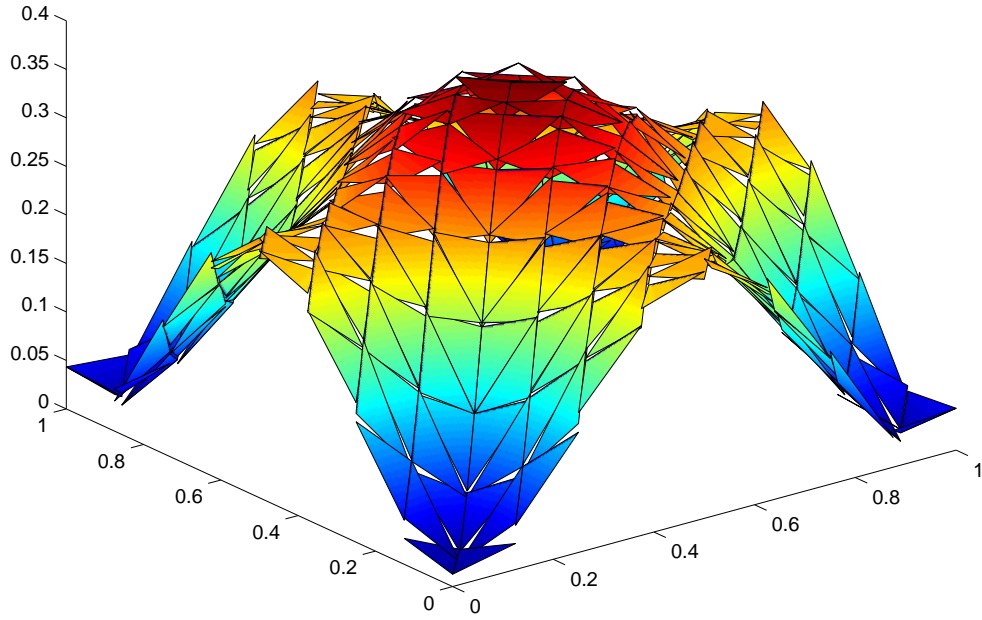


Figure 4.2: Norm of a discrete solution of example (4.10) with $\alpha = 1$

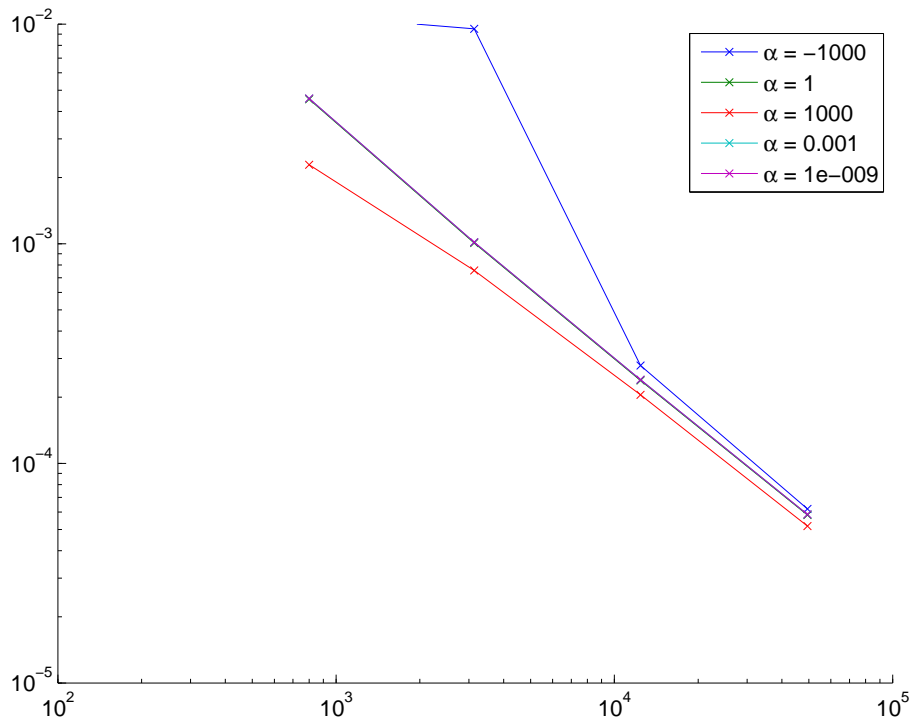


Figure 4.3: L_2 error graph of example (4.10) with uniform refinement

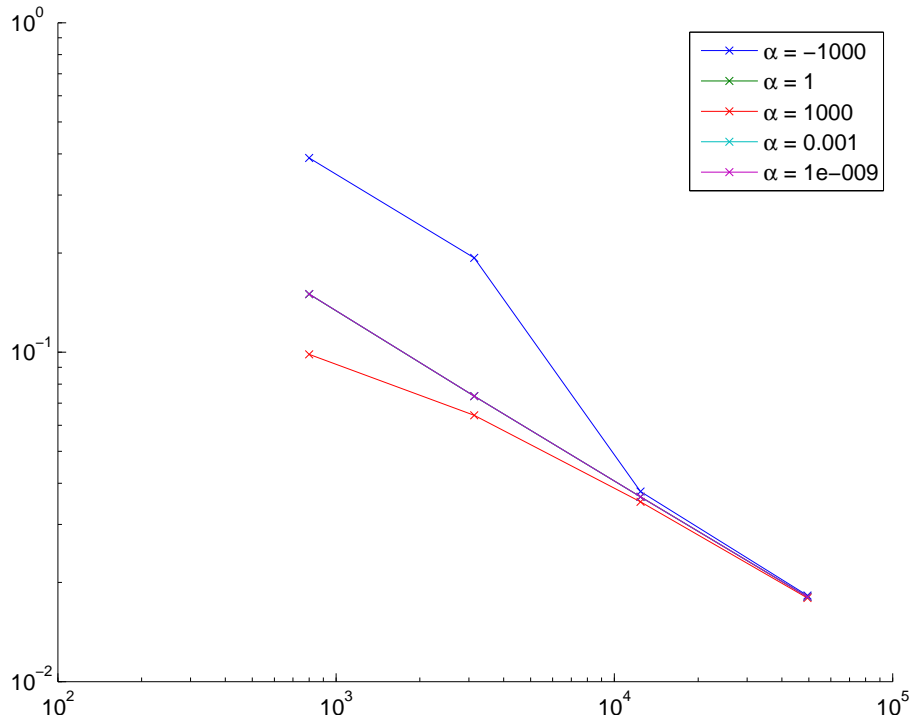


Figure 4.4: Energy error graph of example (4.10) with uniform refinement

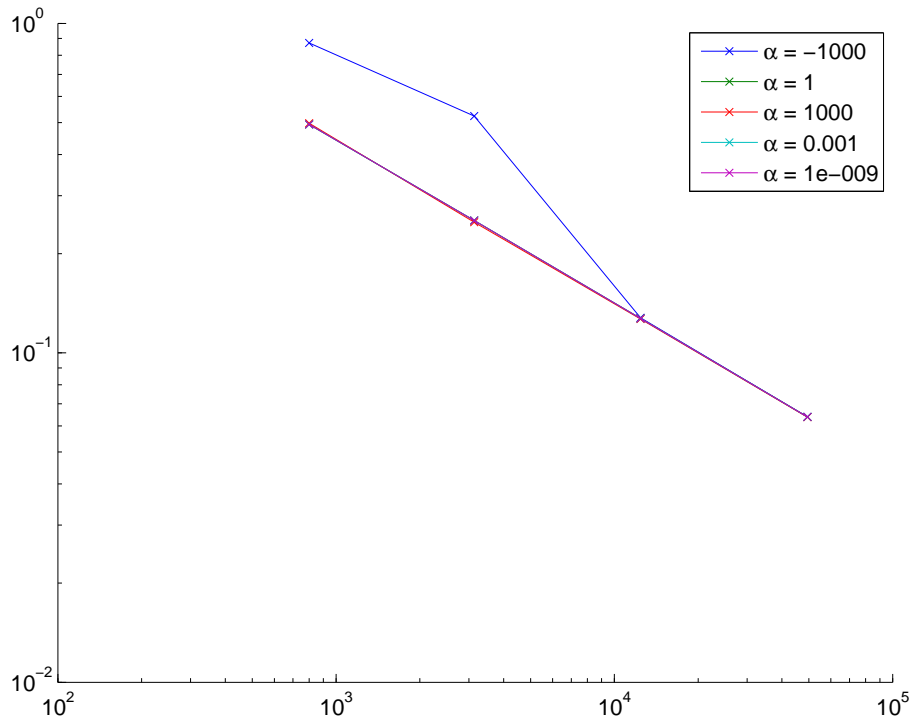


Figure 4.5: Estimated error graph of example (4.10) with uniform refinement

4.3.2 The L-shape domain

Let

$$u = \nabla \times (r^{2/3} \cos(\frac{2}{3}\theta - \frac{\pi}{3})\phi(r)) \quad (4.11)$$

on $\Omega = [-1, 1]^2 \setminus (0, 1)^2$ where (r, θ) are the polar coordinates at the origin and ϕ is a cut-off function which is employed to obtain the zero boundary conditions.

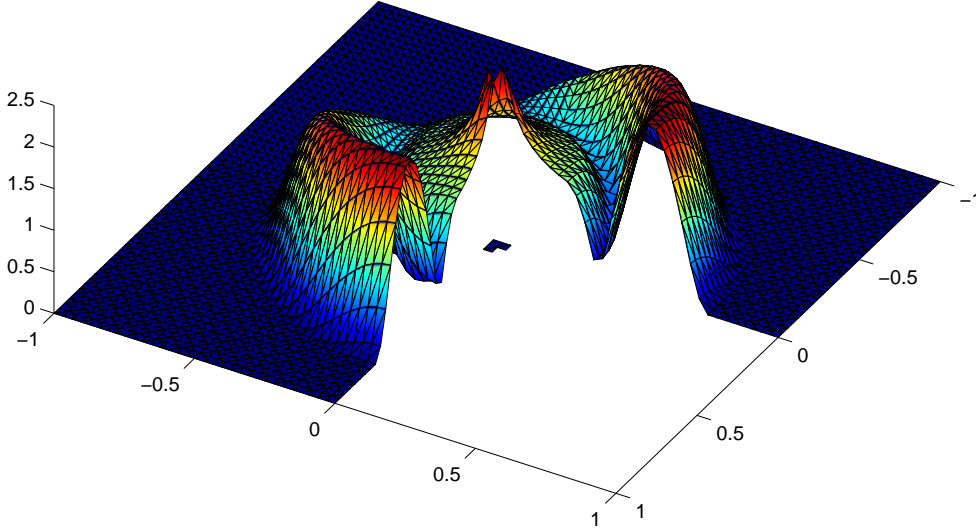


Figure 4.6: Norm of the exact solution of example (4.11)

Uniform refinement seems to result in optimal convergence (see figures 4.8 and 4.9) rates which it should not, as the function u cannot be approximated optimally by uniform meshes. The reason for this is that the cut-off function ϕ introduces a large curl in the interior of the domain (see figures 4.6 and 4.18) which dominates the error for coarse meshes, but can be reduced optimally with uniform refinement. The last refinement step hints at the suboptimal convergence of uniform refinement in this example.

The adaptive results for this solution show a fundamental problem when we compute solutions for large negative parameters α , e.g. $\alpha = -100$ (see figures 4.15 and 4.16). One result of chapter 3 was, that we need $h < h^*$ for some unknown mesh parameter h^* . As long as $h \geq h^*$ we do not have any error reduction. Once h is small enough, the error converges optimally. To cure this behavior one has to start the adaptive algorithm with a mesh that is fine enough.

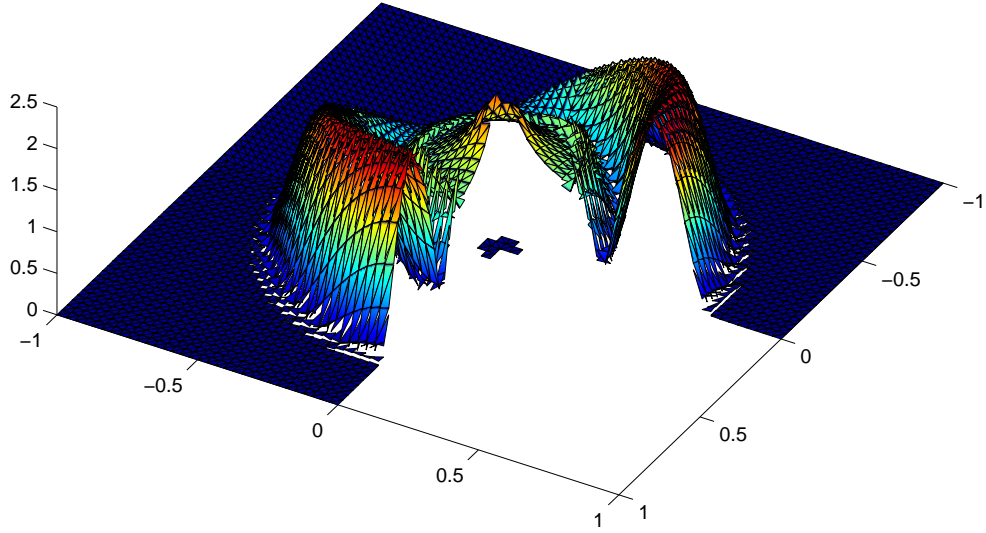


Figure 4.7: Norm of a discrete solution of example (4.11) with $\alpha = 1$

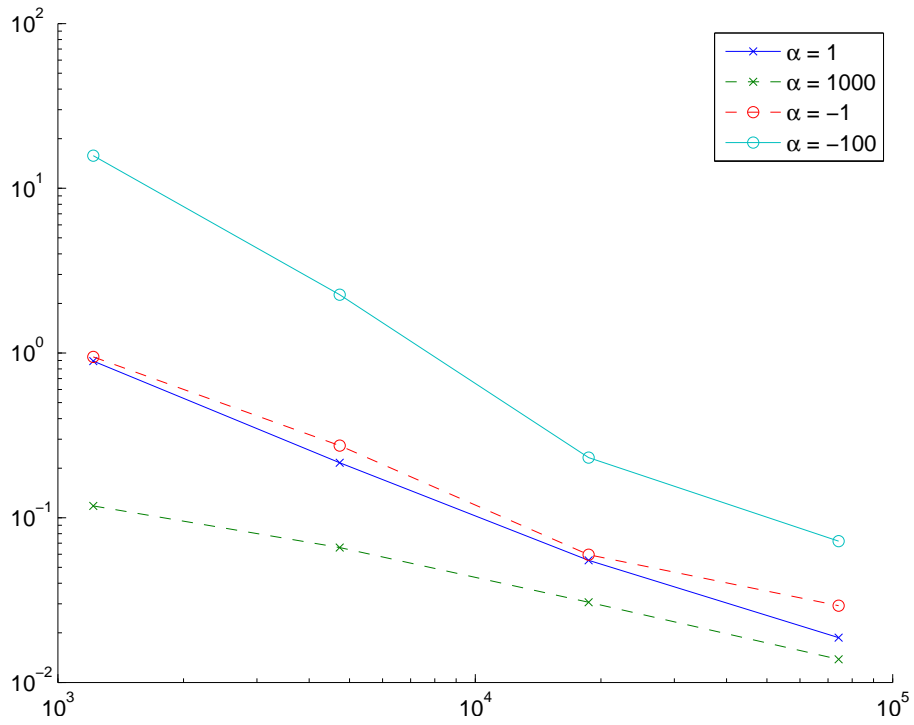


Figure 4.8: L_2 error graph of example (4.11) with uniform refinement

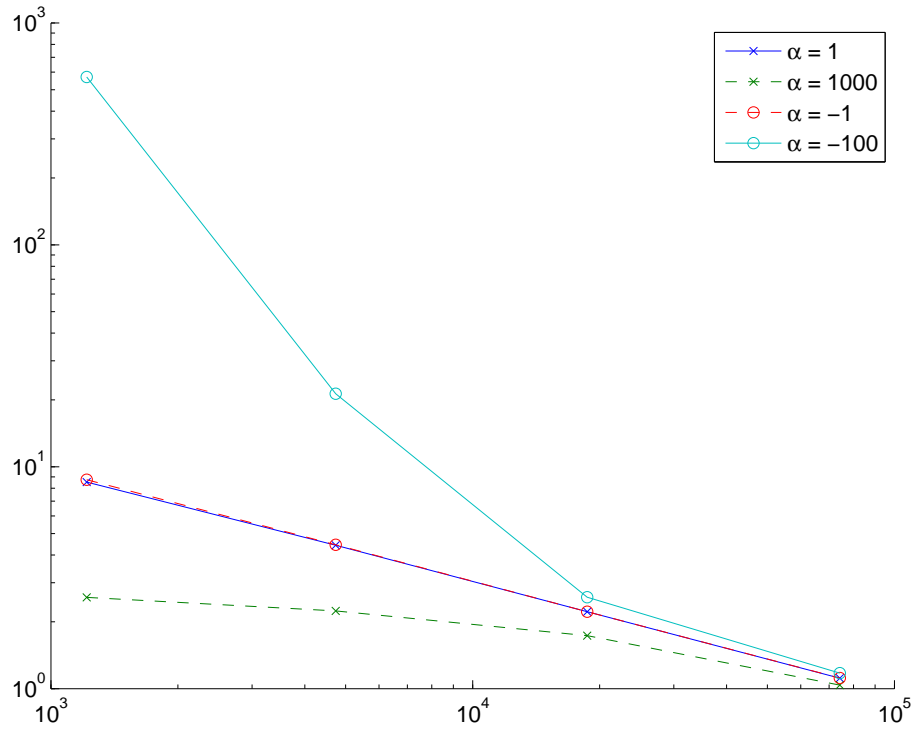


Figure 4.9: Energy error graph of example (4.11) with uniform refinement

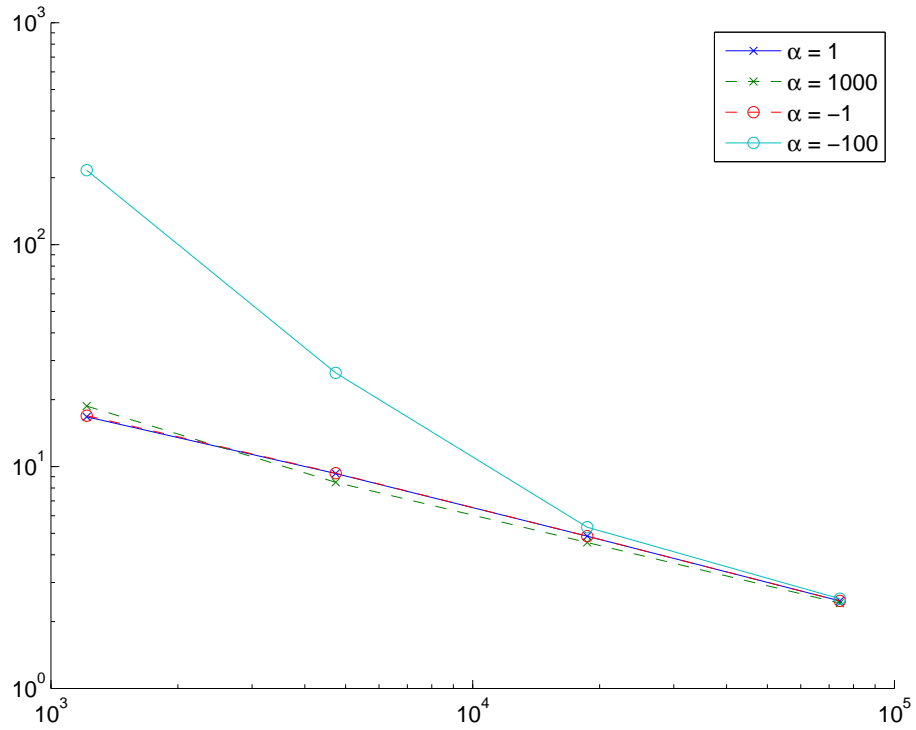


Figure 4.10: Estimated error graph of example (4.11) with uniform refinement

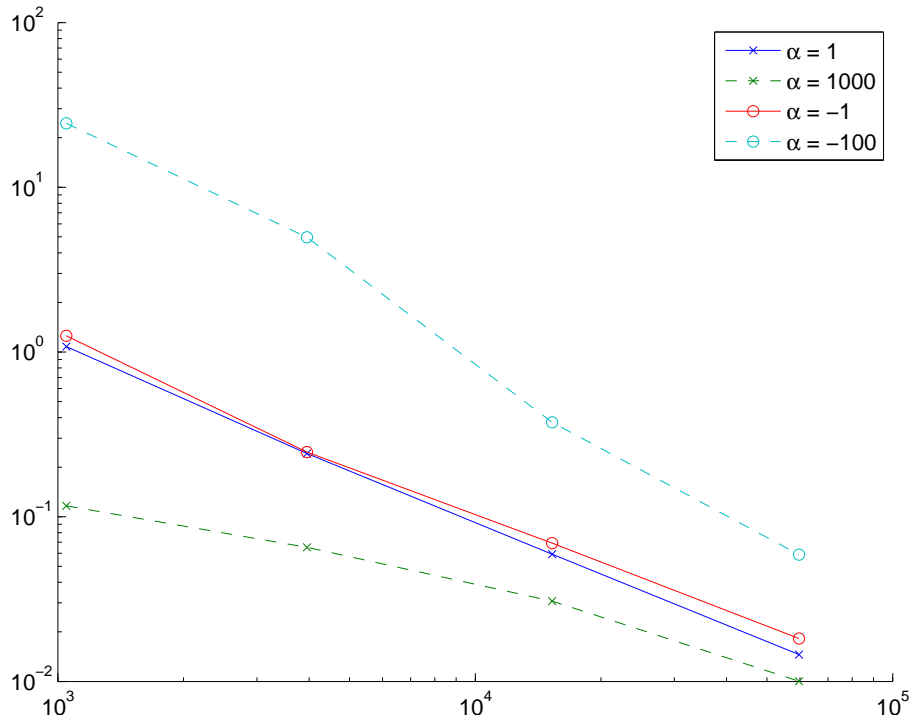


Figure 4.11: L_2 error graph of example (4.11) on graded meshes

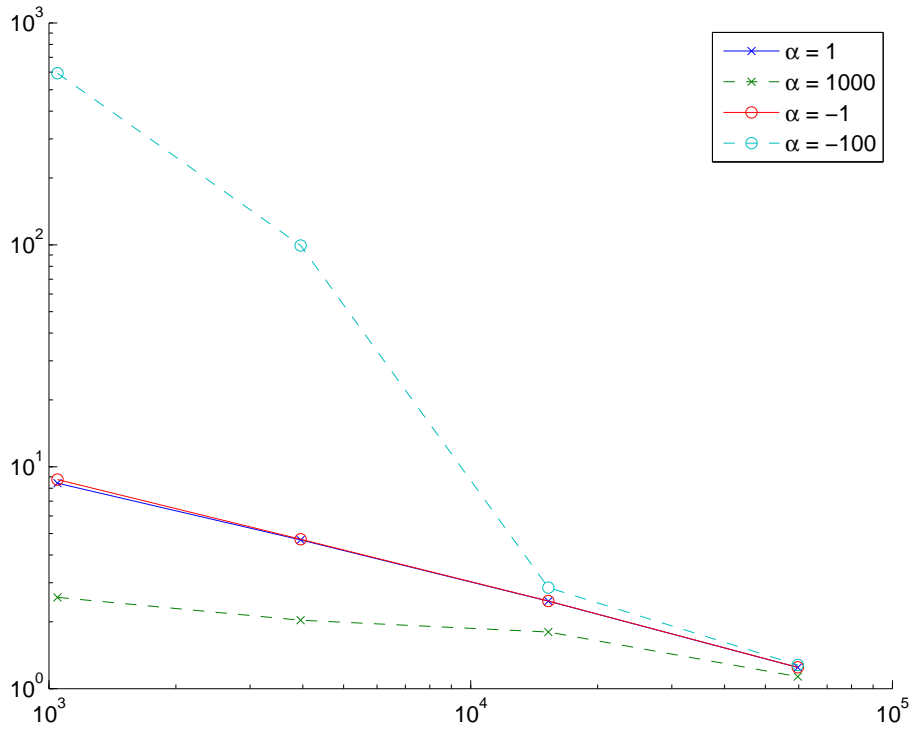


Figure 4.12: Energy error graph of example (4.11) on graded meshes

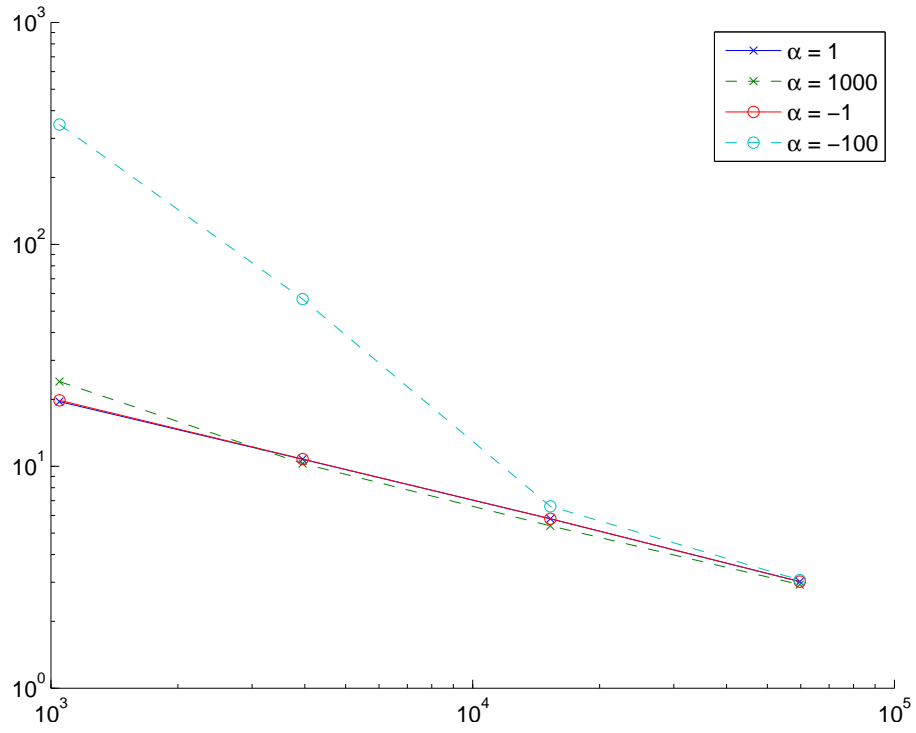


Figure 4.13: Estimated error graph of example (4.11) on graded meshes

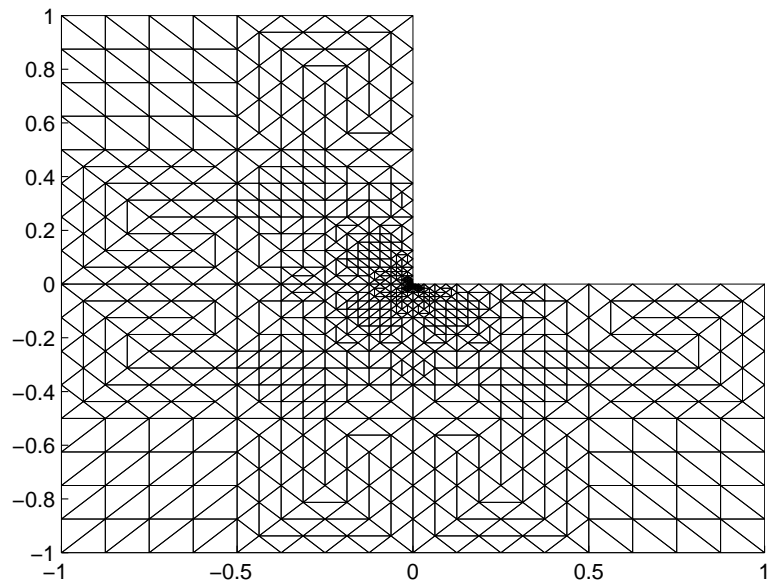


Figure 4.14: One of the graded meshes used for example (4.11)

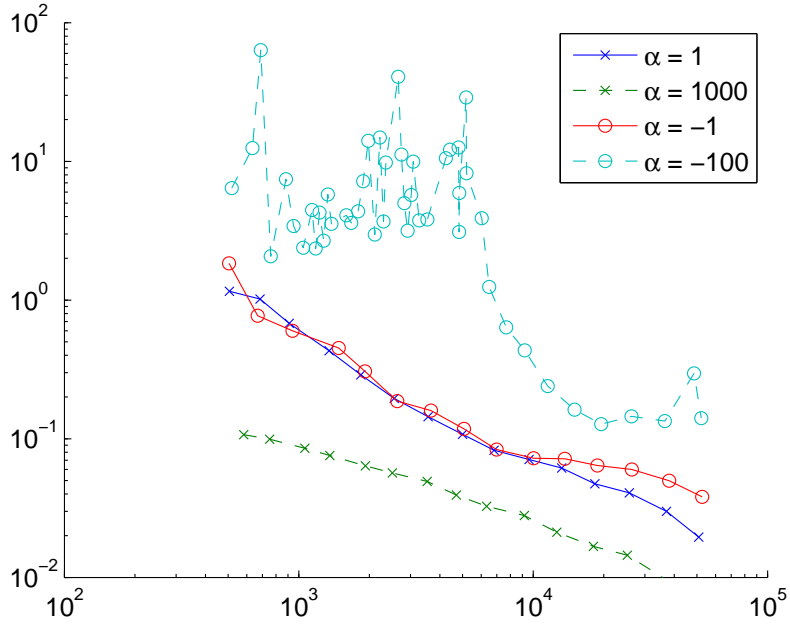


Figure 4.15: L_2 error graph of example (4.11) on graded meshes

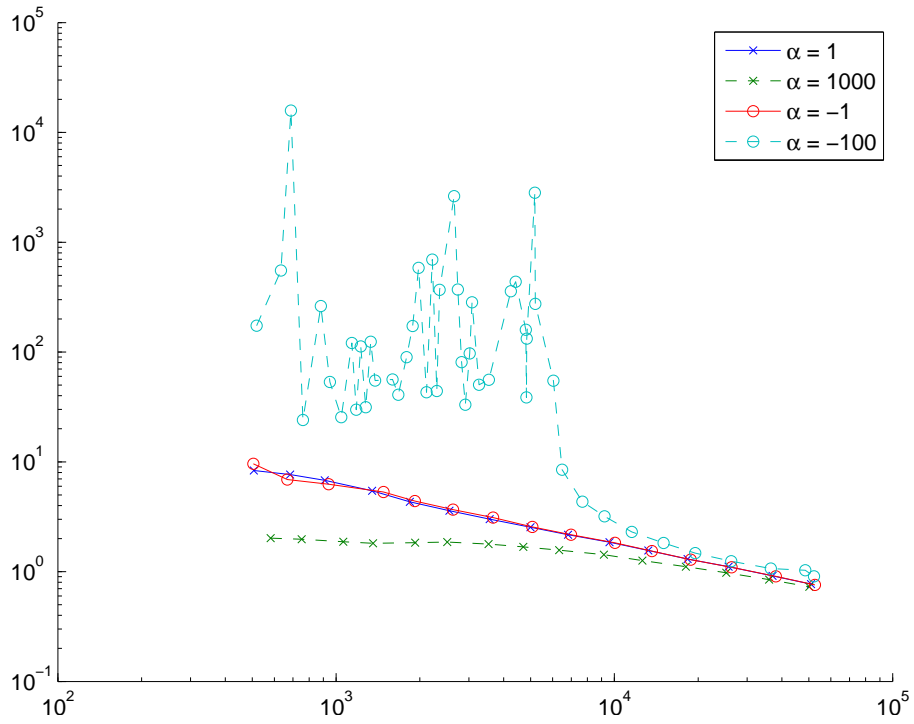


Figure 4.16: Energy error graph of example (4.11) on graded meshes

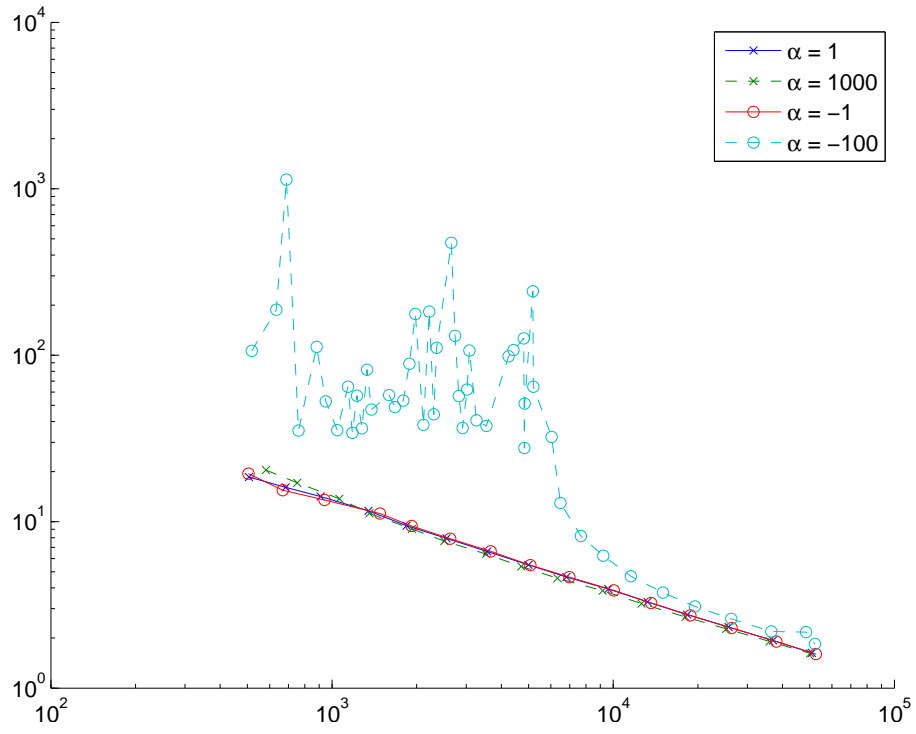


Figure 4.17: Estimated error graph of example (4.11) on graded meshes

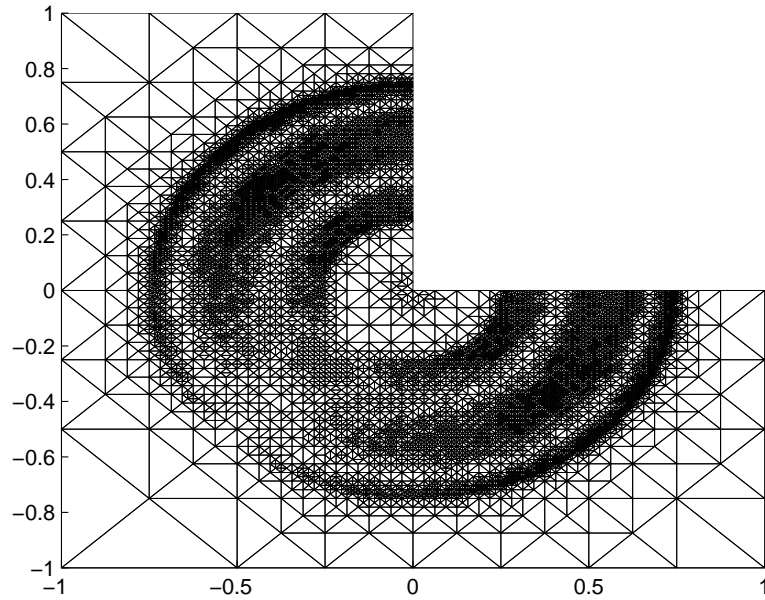


Figure 4.18: One of the adaptive meshes used for example (4.11) generated by the error estimator

To illustrate the suboptimal convergence rate of uniform refinement we compute the solution on the L-shape domain with a right hand side

$$f \equiv 1 \tag{4.12}$$

and zero boundary data (see figure 4.19 for a discrete solution). We only plot the estimated error as the exact solution is unknown in this case. In figure 4.20 one can clearly see the suboptimal convergence on uniform meshes.

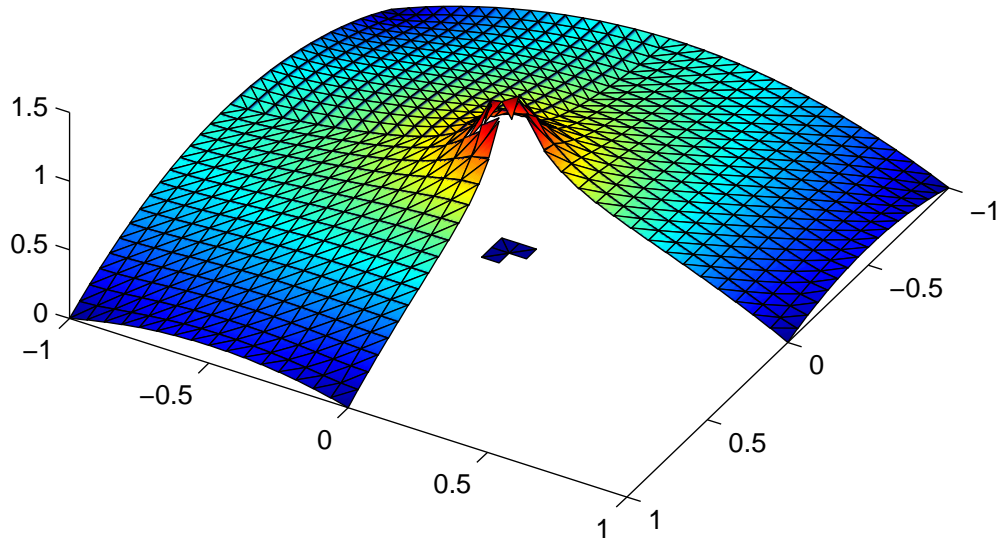


Figure 4.19: Norm of the exact solution of example (4.12)

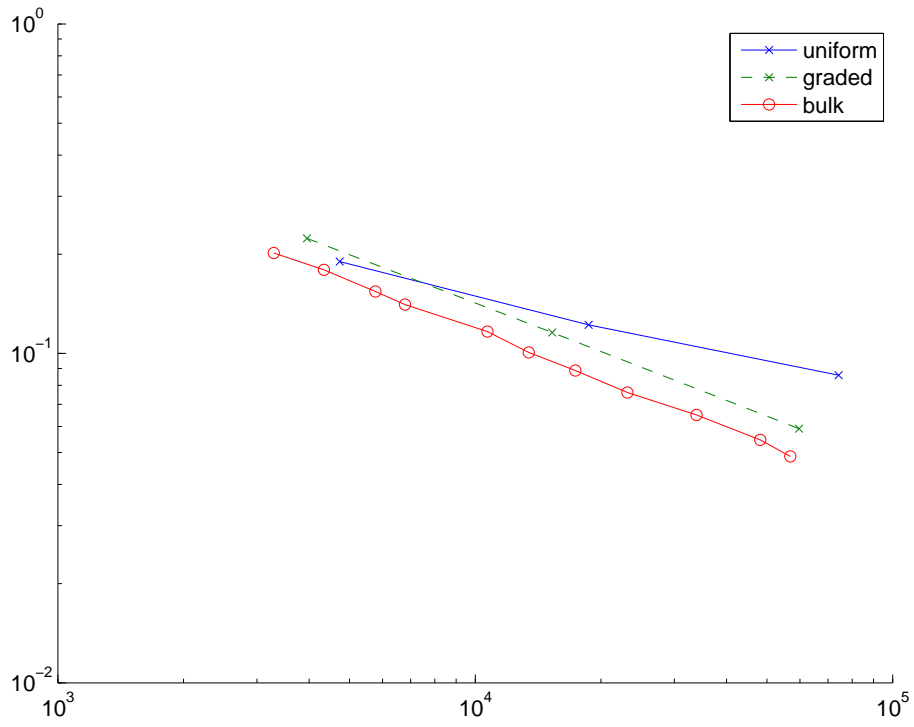


Figure 4.20: Estimated error graph of example (4.12) on graded meshes

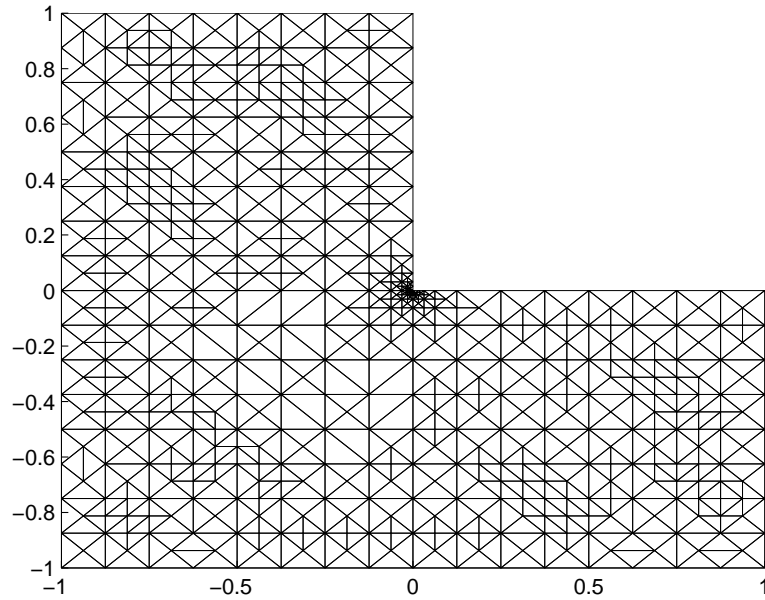


Figure 4.21: One of the adaptive meshes used for example (4.12) generated by the error estimator

4.3.3 The half-L-shape domain

Let

$$u = \nabla \times (r^{4/3} \cos(\frac{4}{3}\theta - \frac{4\pi}{3})\phi(r)) \quad (4.13)$$

on $\Omega = \text{conv}\{(0,0), (-1,0), (-1,-1), (1,-1)\}$ (see figure 4.22 for a discretization of the domain) where (r, θ) are the polar coordinates at the origin and ϕ is a cut-off function which is employed to obtain the zero boundary conditions.

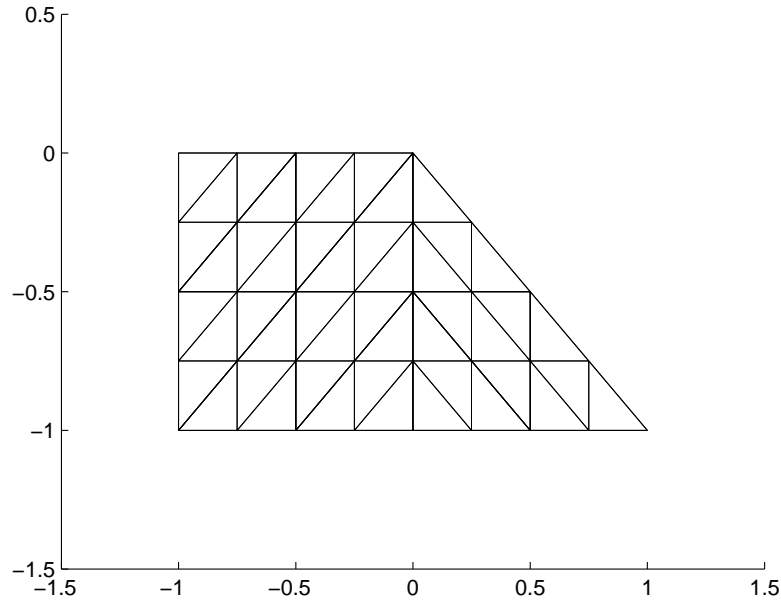


Figure 4.22: A discretization of the half-L-shape domain

The numerical results for this example all exhibit optimal convergence behavior (see figures 4.23 and 4.24). The reason for this seems to be the same as for the L-shape domain with an exact solution, i.e. the cut-off function lets the error in the regular part of the solution dominate the error in the irregular part. As the singularity is less severe in this example, a suboptimal convergence behavior is not even hinted at.

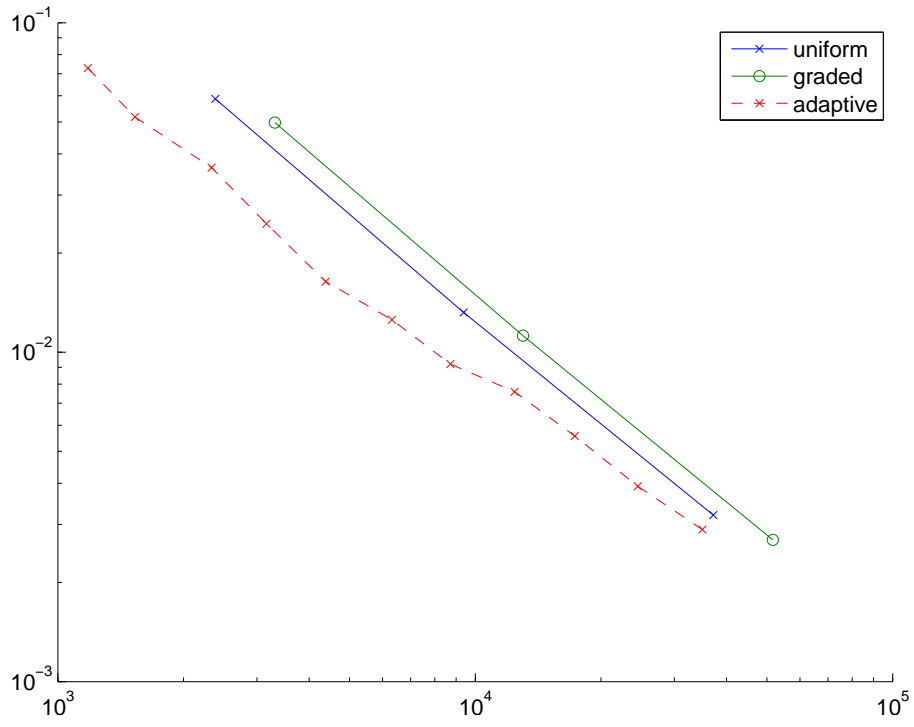


Figure 4.23: L_2 error graph of example (4.13) with $\alpha = 1$

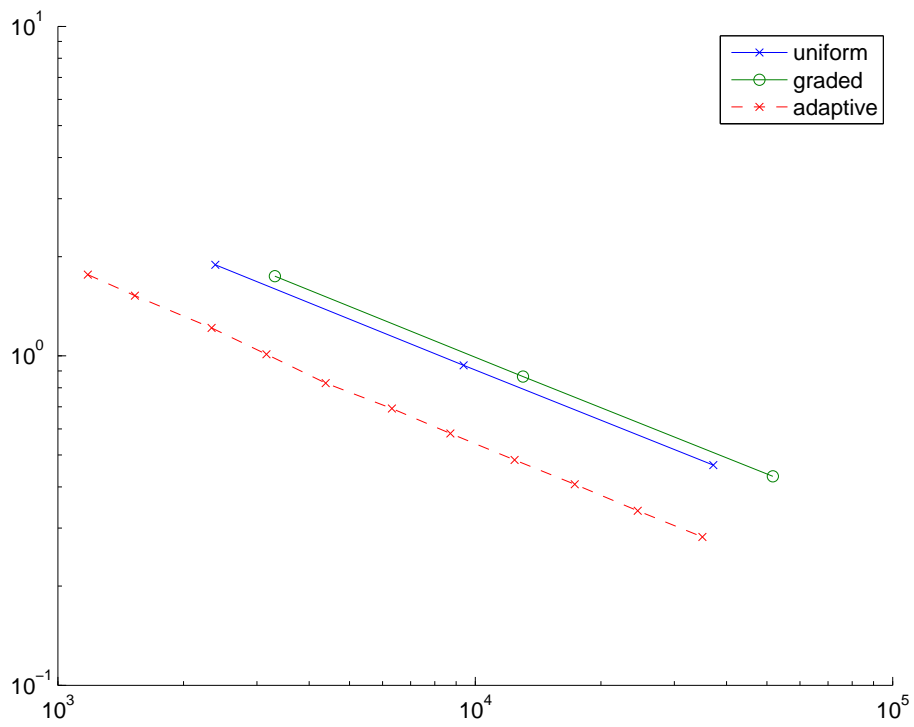


Figure 4.24: Energy error graph of example (4.13) with $\alpha = 1$

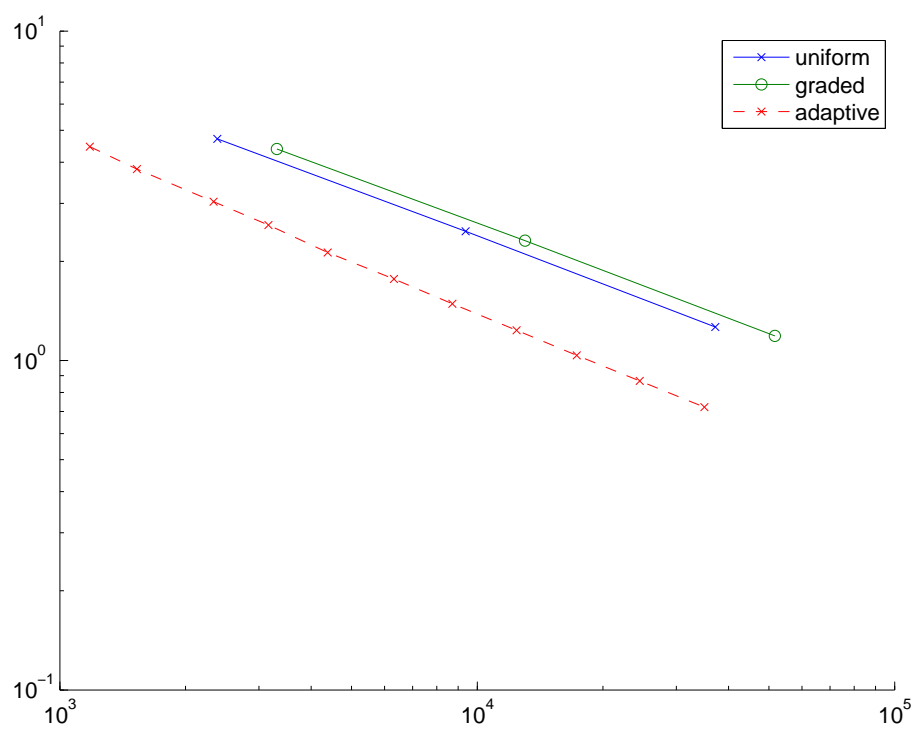


Figure 4.25: Estimated error graph of example (4.13) with $\alpha = 1$

To show that grading or adaptivity can be necessary to obtain optimal convergence on convex domains when one computes solutions for Maxwell's equations we compute the discrete solution to (4.13) without the cut off function, i.e. we now set

$$u = \nabla \times (r^{4/3} \cos(\frac{4}{3}\theta - \frac{4\pi}{3})). \quad (4.14)$$

Note that we now have a non homogeneous boundary which is not covered by the theory of chapter 3. The error graphs for this example show the expected sub optimal convergence order on uniform meshes (see figures 4.26 and 4.27), while the method converges optimally when one uses graded meshes or employs the error estimator as a local mesh refinement indicator.

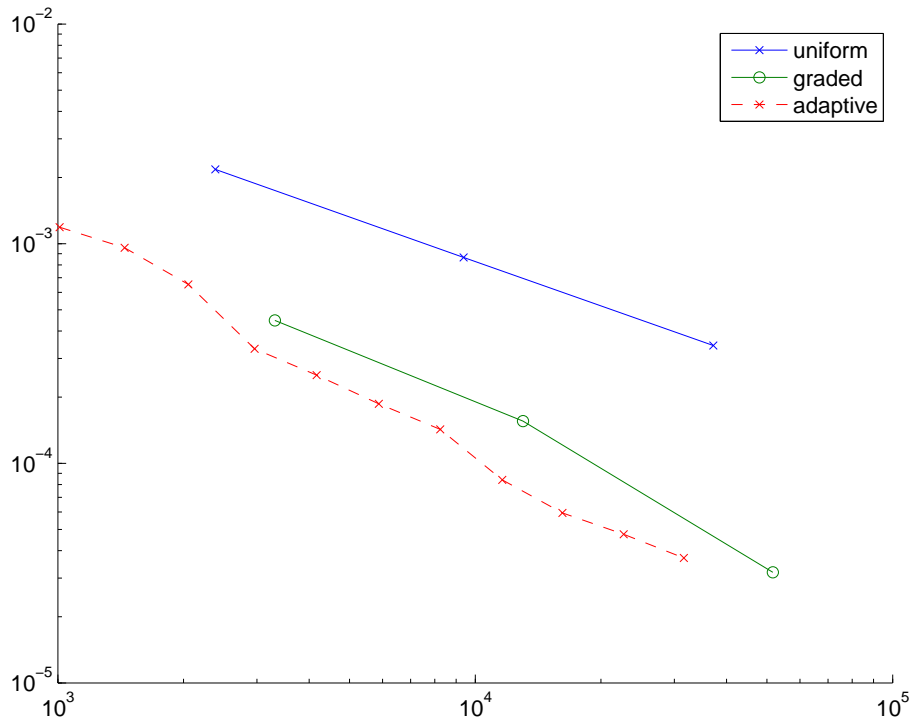


Figure 4.26: L_2 error graph of example (4.14) with $\alpha = 1$

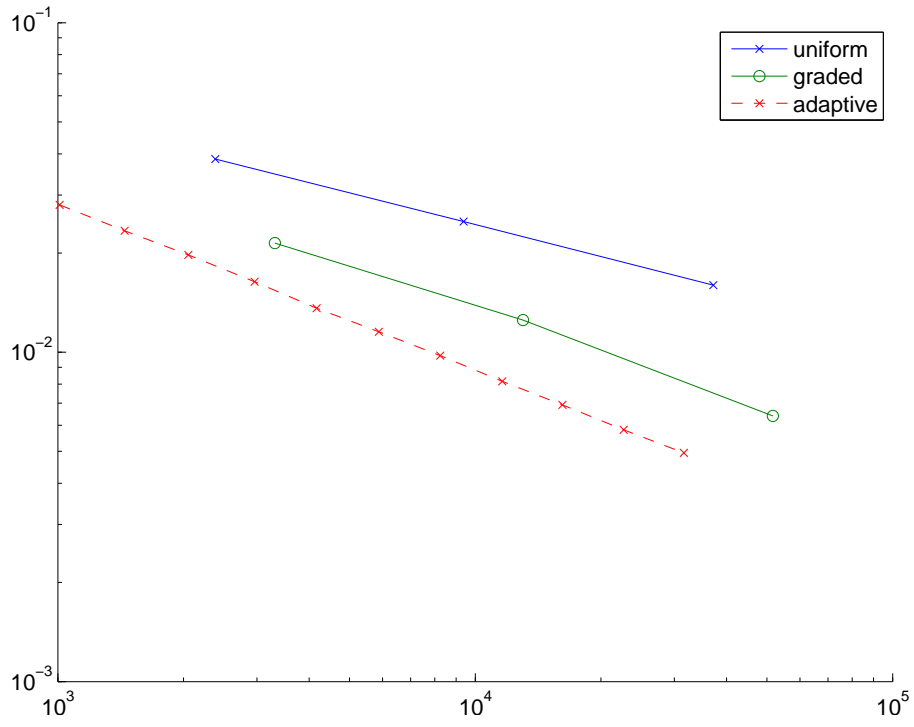


Figure 4.27: Energy error graph of example (4.14) with $\alpha = 1$

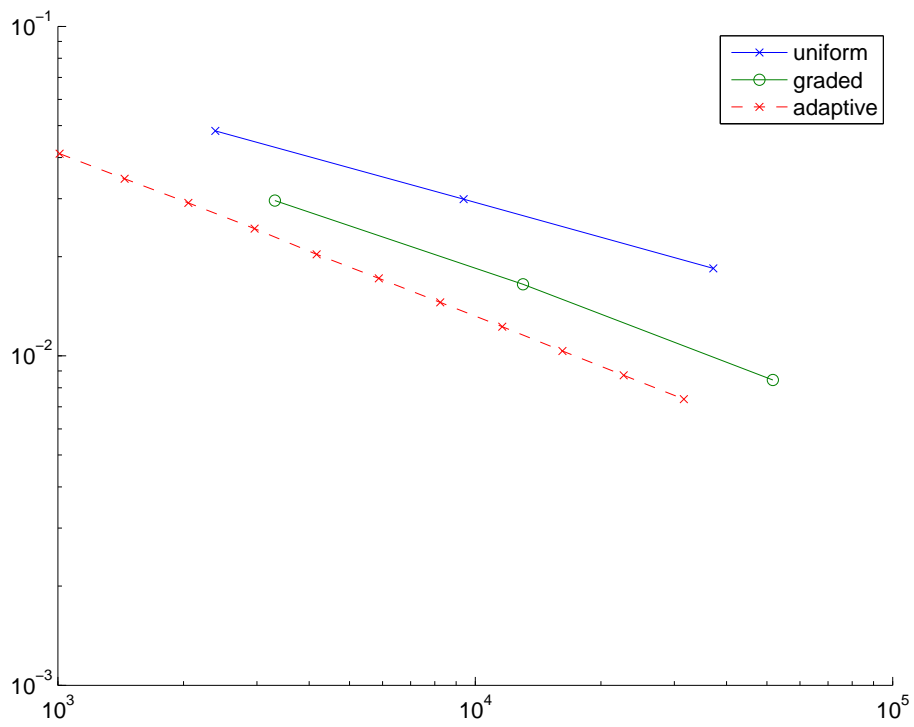


Figure 4.28: Estimated error graph of example (4.14) with $\alpha = 1$

For the last example we compute a discrete solution on the half-L-shape domain with

$$f \equiv 1 \quad (4.15)$$

and zero boundary data (see figure 4.29 for a discrete solution). This example shows that the regular part of the solution can dominate the irregular part pre-asymptotically for constant right hand sides. In practice one may therefore not notice an immediate improvement when one uses graded meshes.

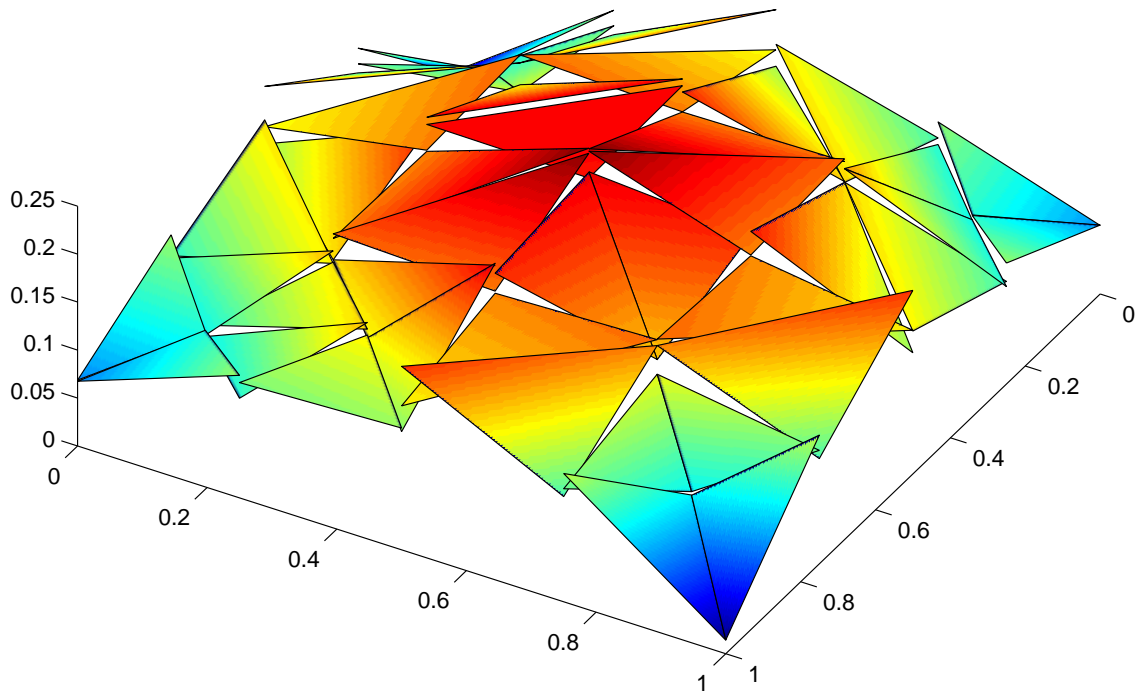


Figure 4.29: Norm of a discrete solution of example (4.15)

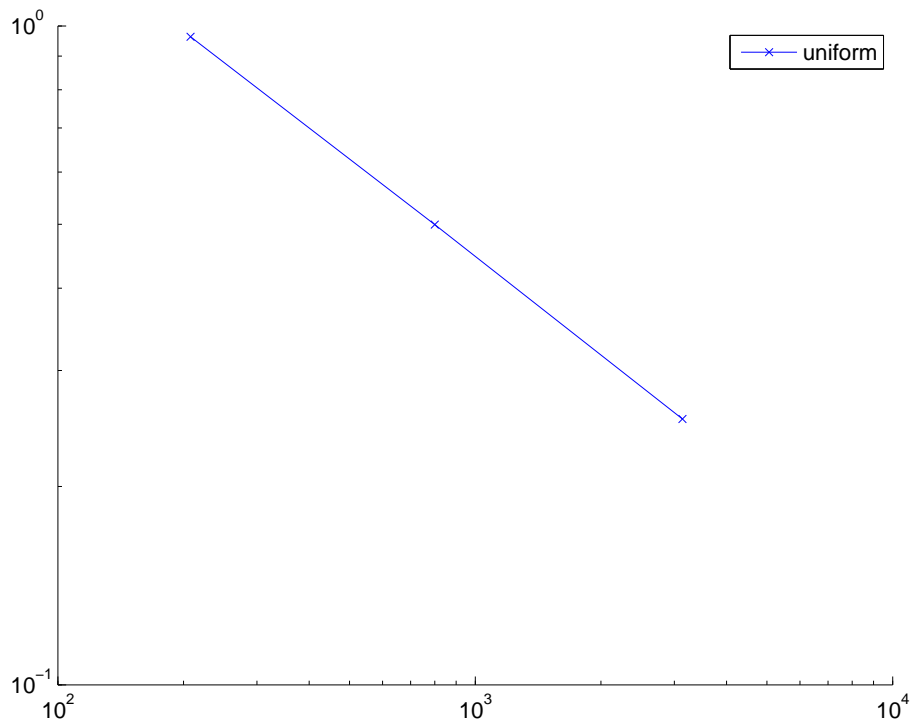


Figure 4.30: Estimated error graph of example (4.15) on graded meshes

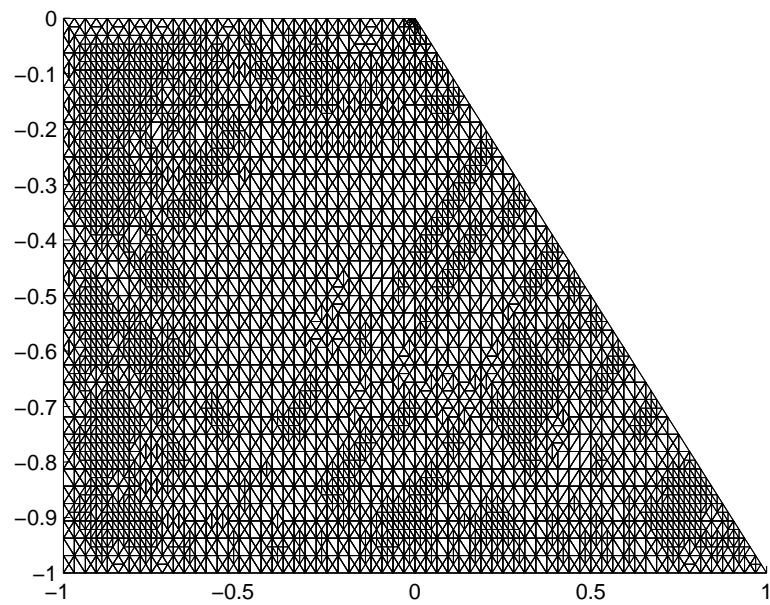


Figure 4.31: One of the adaptive meshes used for example (4.15) generated by the error estimator

Bibliography

- [1] S.C. Brenner, F.Li, and L.-Y. Sung., A locally divergence-free nonconforming finite element method for the time harmonic Maxwell equations. *Math. Comp.*, 76:573, 2007.
- [2] S.C. Brenner, F.Li, and L.-Y. Sung., A nonconforming finite element method for a two dimensional curl-curl minus grad-div problem. (in preparation).
- [3] P. Monk. *Finite Element Methods for Maxwell's Equations*. Oxford University Press, New York, 2003.

Selbstständigkeitserklärung

Ich erkläre, dass ich die vorliegende Arbeit selbständig und nur unter Verwendung der angegebenen Literatur und Hilfsmittel angefertigt habe.

Berlin, den 29.6.2007

Unterschrift

Einverständniserklärung

Hiermit erkläre ich mich einverstanden, dass ein Exemplar meiner Diplomarbeit in der Bibliothek des Institutes für Mathematik verbleibt.

Berlin, den 29.6.2007

Unterschrift

Chapter 5

Theses

- (a) For the solution of Maxwell's equations a converging method was motivated and presented.
- (b) The result that this method converges optimally even for non convex domains was presented.
- (c) It was shown that this method can be efficiently implemented.
- (d) A plausible error estimator has been proposed which seems to be reliable and efficient in practice and produces a sequence of meshes such that the method converges optimally. The reliability and efficiency has still to be established. However, since the solution is generally not in $H(\nabla; \Omega)$, it is conjectured that new techniques and ideas will have to be developed to show this on general domains.
- (e) It was demonstrated, that a theoretical result for the indefinite case (i.e. one only has an estimate for all $h < h^*$ for some mesh granularity h^*) induces some difficulty for the adaptive method. The adaptive algorithm should only be employed if $h < h^*$. The best way to deal with this problem in practice is not clear yet.